doi:10.1016/S0022-2836(02)00328-5 available online at http://www.idealibrary.com on IDEAL® J. Mol. Biol. (2002) 319, 615–635

JMB

Biophysical Studies of eIF4E Cap-binding Protein: Recognition of mRNA 5′ Cap Structure and Synthetic Fragments of eIF4G and 4E-BP1 Proteins

Anna Niedzwiecka[1], Joseph Marcotrigiano[2], Janusz Stepinski[1] Marzena Jankowska-Anyszka[3], Aleksandra Wyslouch-Cieszynska[4] Michal Dadlez[1,4], Anne-Claude Gingras[5], Pawel Mak[6] Edward Darzynkiewicz[1], Nahum Sonenberg[5], Stephen K. Burley[2,7] and Ryszard Stolarski[1]*

[1]*Department of Biophysics Institute of Experimental Physics, Warsaw University 93 Zwirki & Wigury Street 02-089 Warszawa, Poland*

[2]*Laboratories of Molecular Biophysics, The Rockefeller University, New York, NY 10021, USA*

[3]*Faculty of Chemistry Warsaw University 02-093 Warszawa, Poland*

[4]*Institute of Biochemistry and Biophysics, Polish Academy of Sciences, 02-106 Warszawa Poland*

[5]*Department of Biochemistry and McGill Cancer Center McGill University, Montreal Quebec, H3G 1Y6 Canada*

[6]*Institute of Molecular Biology and Biotechnology, Jagiellonian University, 30-387 Krakow Poland*

[7]*Howard Hughes Medical Institute, The Rockefeller University, New York NY 10021, USA*

**Corresponding author*

mRNA 5′-cap recognition by the eukaryotic translation initiation factor eIF4E has been exhaustively characterized with the aid of a novel fluorometric, time-synchronized titration method, and X-ray crystallography. The association constant values of recombinant eIF4E for 20 different cap analogues cover six orders of magnitude; with the highest affinity observed for m^{7}GTP ($\sim 1.1 \times 10^8\ M^{-1}$). The affinity of the cap analogues for eIF4E correlates with their ability to inhibit *in vitro* translation. The association constants yield contributions of non-covalent interactions involving single structural elements of the cap to the free energy of binding, giving a reliable starting point to rational drug design. The free energy of 7-methylguanine stacking and hydrogen bonding (-4.9 kcal/mol) is separate from the energies of phosphate chain interactions (-3.0, -1.9, -0.9 kcal/mol for α, β, γ phosphates, respectively), supporting two-step mechanism of the binding. The negatively charged phosphate groups of the cap act as a molecular anchor, enabling further formation of the intermolecular contacts within the cap-binding slot. Stabilization of the stacked Trp102/m^{7}G/Trp56 configuration is a precondition to form three hydrogen bonds with Glu103 and Trp102. Electrostaticly steered eIF4E-cap association is accompanied by additional hydration of the complex by approximately 65 water molecules, and by ionic equilibria shift. Temperature dependence reveals the enthalpy-driven and entropy-opposed character of the m^{7}GTP–eIF4E binding, which results from dominant charge-related interactions ($\Delta H^\circ = -17.8$ kcal/ mol, $\Delta S^\circ = -23.6$ cal/mol K). For recruitment of synthetic eIF4GI, eIF4GII, and 4E-BP1 peptides to eIF4E, all the association constants were $\sim 10^7\ M^{-1}$, in decreasing order: eIF4GI > 4E-BP1 > eIF4GII ~ 4E-BP1 (P-Ser65) ~4E-BP1(P-Ser65/Thr70). Phosphorylation of 4E-BP1 at Ser65 and Thr70 is insufficient to prevent binding to eIF4E. Enhancement of the eIF4E affinity for cap occurs after binding to eIF4G peptides.

Keywords: eIF4E; mRNA 5′ cap; translation; structure–activity relationship; fluorescence

Present address: J. Marcotrigiano, Laboratory of Virology and Infectious Disease, The Rockefeller University, New York, NY 10021, USA.

Abbreviations used: 2′OmG, 2′-*O*-methylguanosine; 4E-BP1, 4E binding protein 1, also called phosphorylated heat- and acid-stable protein regulated by insulin (PHAS-I); bz^{7}GTP, 7-benzylguanosine 5′-triphosphate; eIF4E, eukaryotic initiation factor 4E; eIF4G, eukaryotic initiation factor 4G, also called p220 or eIF4γ; et^{7}GTP, 7-ethylguanosine 5′-triphosphate; m$_2^{2,7}$GTP, N^2,7-dimethylguanosine 5′-triphosphate; m$_3^{2,2,7}$GTP, N^2,N^2,7-trimethylguanosine 5′-triphosphate; m^{7}G, 7-methylguanosine; m^{7}GDP, 7-methylguanosine 5′-diphosphate; m^{7}GMP, 7-methylguanosine 5′-monophosphate; m^{7}GpppG, P^1-7-methylguanosine-5′ P^3-guanosine-5′ triphosphate and similarly other dinucleoside triphosphates and tetraphosphates; m^{7}GTP, 7-methylguanosine 5′-triphosphate; p, PO_3^-; *p*-Cl-bz^{7}GTP, 7-(*p*-chlorobenzyl)-guanosine 5′-triphosphate; TST, time-synchronized titration.

E-mail address of the corresponding author: stolarsk@biogeo.uw.edu.pl

0022-2836/02/$ - see front matter

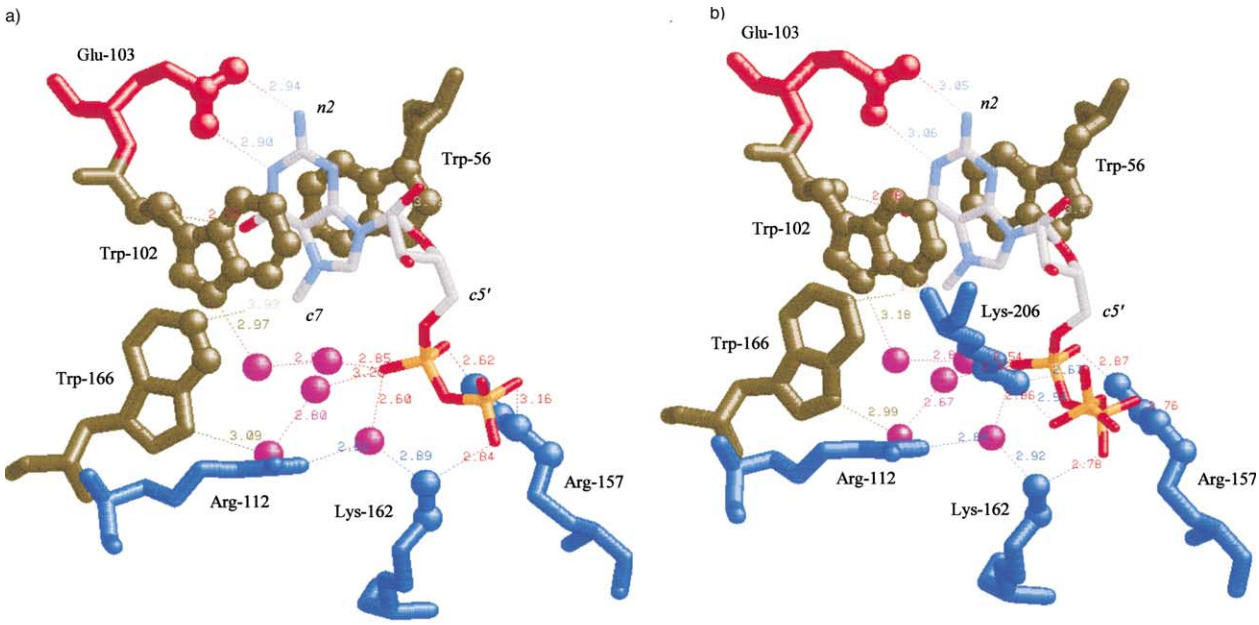

Figure 1. Interatomic contacts in (a) m^{7}GDP-eIF4E complex, determined on the basis of the crystallographic structure (PDB accession no: 1EJ1),[11] and (b) m^{7}GpppG–eIF4E complex. Hydrogen bonds, salt bridges and van der Waals interactions are indicated with dotted lines, with the lengths expressed in Å. Trapped water molecules supporting the hydrogen-bonded network are shown as magenta spheres. The fragments of eIF4E distant from the cap by ≤4 Å are shown as spheres.

Introduction

All nuclear transcribed mRNAs possess a 5′-terminal "cap", m^{7}GpppN, in which 7-methylguanosine is linked by a 5′-5′-triphosphate bridge to the first nucleoside. The cap structure is necessary for optimal mRNA translation,[1,2] participates in the splicing of mRNA precursors,[3,4] and affects nuclear export and mRNA stability.[5] The cap function in translation is mediated by the 25 kDa protein eukaryotic initiation factor 4E (eIF4E), a phylogenetically highly conserved subunit of the heterotrimeric eIF4F initiation complex.[6] In higher eukaryotes eIF4F consists of eIF4E, eIF4A, an RNA helicase, and eIF4G, an adaptor protein.[6–8] Two isoforms of eIF4G, namely eIF4GI (171 kDa)[9] and eIF4GII (176 kDa)[10] are present in mammals. These scaffolding molecules act as a molecular bridge between eIF4E and eIF4A.[7,10] The eIF4Gs interact with the ribosome-bound multisubunit factor eIF3, to recruit the 40 S ribosomal subunit. Additional interaction of the eIF4Gs with the poly(A)-binding protein (PABP) allows for mRNA circularization.[6,8]

Three-dimensional structures of murine eIF4E and its yeast homologue, both bound to 7-methyl-GDP, were solved by X-ray crystallography[11] and by solution NMR spectroscopy,[12] respectively. The complex is shaped like a cupped hand, with the cap analogue located in a narrow cap-binding slot on the concave surface of the protein. Recognition of the 7-methylguanine moiety is mediated by base sandwich-stacking between Trp56 and Trp102 (Figure 1(a)), formation of three Watson–Crick-like hydrogen bonds with a side-chain carboxylate of a conserved Glu103 and a backbone NH of Trp102, and a van der Waals contact of the N(7)-methyl group with Trp166. The diphosphate chain forms salt bridges and direct or water-mediated hydrogen bonds with the NH of Trp102 and Trp166 indole rings, and side-chains of Arg112, Lys162, and Arg157. A new crystallographic structure of a complex of eIF4E bound to the dinucleotide cap analogue, m^{7}GpppG, is discussed herein (Figure 1(b)).

While the structure determinations provided important information on the mode of cap binding, the consistent energetic description of the cap–eIF4E interaction was still lacking. Measurements in solution are necessary to address the mechanistic bases of complex formation and stability. eIF4E possesses eight tryptophan residues which are conserved both in number and location,[2] and cap binding results in quenching of the intrinsic protein fluorescence.[13–20] However, previous fluorescence measurements of the interaction between cap analogues and eIF4E purified by m^{7}G-affinity chromatography yielded puzzling data. The reported association constants,[14–18] in the range of 10^5–10^6 M^{-1}, did not reflect the differing inhibitory potency of cap analogues observed *in vitro*,[21] and contrasted with the structural data[11] showing that the binding constant for the eIF4E–m^{7}GDP complex should be a few orders of magnitude higher. These divergences prompted us to perform systematic fluorescence quenching measurements to determine the affinity for cap analogues of recombinant eIF4E, purified without

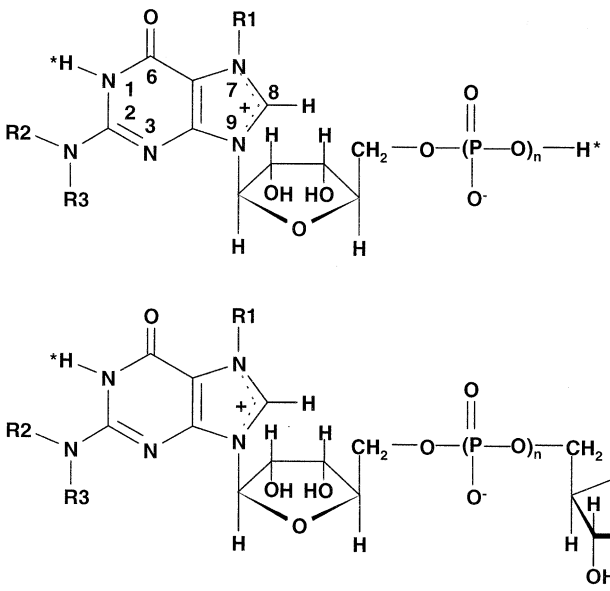

m^7GTP:	$R1 = CH_3$,	$R2 = R3 = H$,	$n = 3$;		
m^7GDP:	$R1 = CH_3$,	$R2 = R3 = H$,	$n = 2$;		
m^7GMP:	$R1 = CH_3$,	$R2 = R3 = H$,	$n = 1$;		
m^7G:	$R1 = CH_3$,	$R2 = R3 = H$,	$n = 0$;		
et^7GTP:	$R1 = CH_2CH_3$,	$R2 = R3 = H$,	$n = 3$;		
bz^7GTP	$R1 = CH_2\Phi$,	$R2 = R3 = H$,	$n = 3$;		
p-Cl-bz^7GTP:	$R1 = CH_2\Phi Cl$,	$R2 = R3 = H$,	$n = 3$;		
$m_2^{2,7}GTP$:	$R1 = CH_3$,	$R2 = CH_3$, $R3 = H$,	$n = 3$;		
$m_3^{2,2,7}GTP$:	$R1 = CH_3$,	$R2 = R3 = CH_3$,	$n = 3$;		
$m^7Gppp2'OmG$:	$R1 = CH_3$,	$R2 = R3 = H$,	$n = 3$,	$R4 = OCH_3$,	$B = G$
m^7GpppG:	$R1 = CH_3$,	$R2 = R3 = H$,	$n = 3$,	$R4 = OH$,	$B = G$
m^7GpppA:	$R1 = CH_3$,	$R2 = R3 = H$,	$n = 3$,	$R4 = OH$,	$B = A$
m^7GpppC	$R1 = CH_3$,	$R2 = R3 = H$,	$n = 3$,	$R4 = OH$,	$B = C$
m^7Gpppm^7G:	$R1 = CH_3$,	$R2 = R3 = H$,	$n = 3$,	$R4 = OH$,	$B = m^7G$
$m^7GppppG$:	$R1 = CH_3$,	$R2 = R3 = H$,	$n = 4$,	$R4 = OH$,	$B = G$
m^7Gpppm^7G:	$R1 = CH_3$,	$R2 = R3 = H$,	$n = 4$,	$R4 = OH$,	$B = m^7G$

Scheme 1. Structures of the 16 methylated cap-analogues. Φ denotes the phenyl ring. Protons which partially dissociate at pH 7.2, are marked with asterisk ($pK_a^{N(1)-H} \sim 7.24–7.54$, depending on R2, R3, and n[48]; $pK_a^{phosph} \sim 6.1–6.5$, depending on n[62]).

application of m^7G-affinity chromatography. We designed a fast and accurate method of time-synchronized titration (TST) to obtain reliable equilibrium association constant values, which are not only relative to one another, but for the first time have an absolute meaning, and thus can be interpreted in terms of the free energy of binding, leading to the mechanism of the eIF4E–mRNA 5′ cap recognition. Here we focused on the association of recombinant untagged murine eIF4E (residues 28–217) with a large series of mono- and dinucleotide cap analogues (Scheme 1), in order to (a) parse the free energy of binding into the contributions of individual structural elements in the cap-binding center, (b) find a thermodynamic origin for the stacking-hydrogen bonding cooperativity, (c) search for conformational changes and water exchange between the complex and bulk solution, and (d) elucidate the role of ionic equilibria and electrostatic interactions in cap–eIF4E recognition.

Translation initiation is a rate-limiting step of gene expression.[22] eIF4E is the least abundant protein initiation factor and its accessibility for the eIF4F complex formation is suspected to regulate ribosome recruitment.[23] The accessibility of eIF4E in mammals is regulated by interactions with small eIF4E-binding proteins, 4E-BP1, 4E-BP2 and 4E-BP3, which prevent productive interactions between eIF4E and eIF4G.[24,25] Sequence analysis of the 4E-BPs and eIF4Gs suggested that these otherwise unrelated protein families have converged on the same eIF4E binding strategy.[25,26] The eIF4E binding site shared between the 4E-BPs and the eIF4Gs is BXX**YDR**X**FL**Φ, where B is a conserved basic residue, X is variable, Φ is a conserved hydrophobic residue, and invariant residues are shown in boldface.[9,10,27,28] Crystal structures of two ternary complexes of eIF4E with 7-methyl-GDP and peptides encompassing the eIF4E binding sites, derived from eIF4GII or 4E-BP1, revealed that both peptides recognize a phylogenetically invariant, partially hydrophobic, partially acidic surface of the convex dorsum of eIF4E in the vicinity of Trp73, and share a common mode of interaction.[29] After hyperphosphorylation, the 4E-BPs are no longer able to bind eIF4E, allowing eIF4F complex formation and translation initiation to proceed.[30] The phosphorylation mechanism was extensively investigated for 4E-BP1, where at least

six phosphorylation sites were mapped: Thr37, Thr46, Ser65, Thr70, Ser83 and Ser112 (numbering for the human protein). Some of the hypo-phosphorylated forms of 4E-BP1 bind to eIF4E, but hyperphosphorylation abrogates the interaction with eIF4E and enables recruitment of eIF4G. The ordered, hierarchical model of phosphate addition to endogenous 4E-BP1, in which phosphorylation of Thr37 and Thr46 is followed by phosphorylation of Thr70 and finally of Ser65,[30,31] is generally accepted, although some points remain controversial.[32–34] At issue is the influence of the Ser65 or combined Ser65/Thr70 phosphorylation on the 4E-BP1 binding to eIF4E.[31,35] Our fluorescence affinity measurements have been extended to include ternary complexes which consist of eIF4E, a cap-analogue, and a synthetic peptide corresponding to the eIF4E recognition motif from the following mammalian proteins: eIF4GI, eIF4GII, 4E-BP1, and 4E-BP1 monophosphorylated at Ser65 and diphosphorylated at Ser65/Thr70. Application of the precise TST method allowed us to test in a quantitative way the effects of phosphorylation at Ser65 and Thr70 on regulation of 4E-BP1 binding to eIF4E, and the putative cooperation between two binding sites of eIF4E.[36–38]

Results and Discussion

Methodological aspects

Biophysical analysis of intermolecular interactions aimed at rational design of therapeutic agents requires reliable measurements of the protein–ligand association in solution as a necessary counterpart to high resolution structural studies. For eIF4E, such consistent information was lacking. The association constants have been changing significantly with each new publication due to several neglected sources of errors, both experimental and numerical. First, the lack of quantitative control of activity of eIF4E[14–18,20] which is highly unstable (instability index > 40[39]). Second, the presence of practically unremovable contamination of affinity-purified eIF4E with the cap-analogue that was used for the elution from the cap-affinity column. Such eIF4E can be up to 60% m^7GTP-bound, even after application of ionic exchange chromatography[40] or repeated buffer exchange on a 5 kDa NMWL filter (data not shown). Third, dilution of a sample in the course of the titration, "inner filter" effect, and contribution of a free ligand to total fluorescence, were only partially eliminated in the previous publications. Dilution was considered in most of them,[14–18] while the inner filter effect and estimated emission of a free ligand were taken into account properly in the single paper.[18] The results of studies on eIF4E fused with GST, which molecular mass is comparable with that of eIF4E, were useful only for qualitative interpretation.[20]

All above-mentioned experimental problems are rigorously analysed in the current work (see Materials and Methods for detail). Purification of eIF4E *via* refolding from inclusion bodies guarantees that the protein is cap-free. Since eIF4E is a non-enzymatic protein, it is impossible to determine the specific activity of each sample from independent experiments. We thus introduce the active protein concentration (P_{act}) as a free parameter in the numerical analysis, what requires a novel, very precise measuring method of fluorescence quenching. Interactions of the apo-protein with cap analogues are studied by the TST, yielding the goodness of fit $R^2 = 0.999–0.9999$, what assures the accuracy enough to extract the lacking information on the actual protein activity from each specific titration. For previously frozen samples of apo-protein, the active fraction decreases down to ~70% or even to ~10%, depending on the sample volume (12 ml to 10 μl, respectively), but K_{as} of the active protein is unaffected. The inactive fraction aggregates and precipitates, in spite of low protein concentration of the stored stock solution (~0.3 mg/ml), the presence of 10% (v/v) glycerol, 0.5 mM EDTA, and flash-freezing. This is in contrast to the cap-saturated eIF4E, which is stabilized by the ligand (Niedzwiecka, unpublished). The experiments reported here are performed with freshly prepared (not frozen) eIF4E, for which the quantity of active protein varies from 80% to 110% (±12%) of the concentration estimated from the absorption spectra.

All fluorescent species in solution are explicitly included in the numerical analysis. The complete overlapping of the absorption spectra for eIF4E and the cap analogues (Figure 2) makes it impossible to excite the protein selectively. The emission spectra are also overlapped, therefore the contribution from the increasing concentration of the free cap analogues to the total fluorescence in

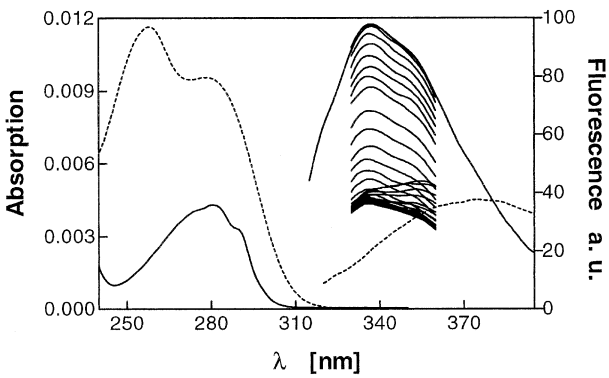

Figure 2. Absorption (left) and fluorescence (right) spectra of eIF4E (continuous line, 0.2 μM) and m^7GTP (broken line, 4 μM) at 20 °C. Typical eIF4E fluorescence quenching spectra upon increasing concentration of m^7GTP (0.7 nM–4 μM). Fluorescence spectra for higher concentrations of m^7GTP exhibit an increasing emission of free m^7GTP present in solution.

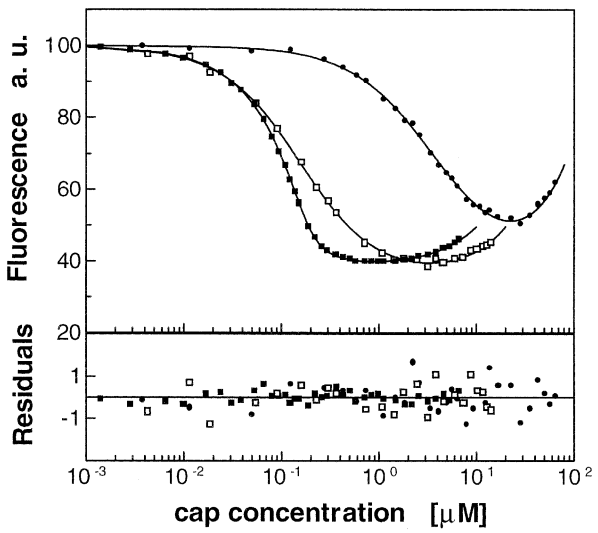

Figure 3. Titration curves for m^7GTP (■), m^7GpppG (□), and $m_3^{2,2,7}$GTP (●) at 20 °C, and fitting residuals. An increasing fluorescence signal at higher cap concentrations originates from the free-cap emission.

the course of the titration must not be neglected. Subtraction of the free cap fluorescence is groundless, since the equilibrium concentration of the free ligand depends on the association constant to be determined. The spectra overlapping leads to erroneous attribution of the signal plateau to the saturation state, while the apparent plateau originates from two effects that cancel each other out: the quenching of the intrinsic protein fluorescence and the increasing emission of the free cap analogues. As a result, the observed maximal fluorescence quenching is different for various cap analogues (Figure 3), and smaller than the calculated intrinsic eIF4E fluorescence quenching (Q, see Materials and Methods), which is the same for different cap analogues (~65%). The association constants determined from the titration curves with the neglected free ligand emission would be erroneous, especially for weakly binding and strongly emitting ligands. Our method of data analysis eliminates these problems. Independently, the previous publications were based mostly on linearised forms of the equilibrium equation[14–18] which are not suitable for the analysis of strong interactions.

The methodological improvements reported herein afford possibilities for a reliable comparison of the results for the protein from different purification batches, previously frozen or not, from experiments at different temperatures, ionic strengths, and pH. The K_{as} values up to $10^8\ M^{-1}$, accompanied by the systematic and self-consistent structure–affinity relationship, provide an exact, quantitative test for the proper fold of the renatured protein. This assures for the first time that the equilibrium association constants reflect the true, intrinsic affinity of eIF4E for mRNA 5′ cap.

Affinity of cap analogues for eIF4E

K_{as} values determined in the present studies (at 20 °C, Hepes/KOH (pH 7.2), 100 mM KCl, 1 mM DTT, 0.5 mM EDTA) varied from $10^8\ M^{-1}$ for specific 7-substituted cap analogues to $10^2\ M^{-1}$ for 7-unsubstituted ligands (Table 1, Scheme 1). The substantial differences of the K_{as} values follow structural modifications of cap, e.g. a 760-fold reduction of K_{as} for $m_3^{2,2,7}$GTP and up to a 5000-fold drop of K_{as} for GTP as compared to m^7GTP. The presence of any N(7)-substituent enhances binding, but the methyl substituent appears to be optimal. Among several elements important for specific eIF4E–cap binding, the negative electrostatic charge of the phosphate chain, which depends both on phosphate number and the presence of a second nucleotide, is of primary importance. The decrease of K_{as} with single stepwise reduction of the phosphate chain in the series of 7-methylated mononucleotides is followed by the same changes of K_{as} for the unmethylated compounds (~five and ~25-fold for removal of the γ-phosphate and the β-phosphate, respectively). Removal of the α-phosphate leads to a drastic fall of K_{as}, which is 175-fold lower for m^7G than that of m^7GMP.

The dinucleotide triphosphate cap analogues also bind to eIF4E less strongly (~20-fold) than m^7GTP. The identity of the second base seems to be of minor importance. Generally, either base of the dinucleotide cap analogues penetrate the binding slot of eIF4E, but since the association constants of unmethylated molecules are far lower than those of the methylated ones, such dual binding is negligible for asymmetrical cap analogues. By contrast, for symmetrical molecules (m^7Gpppm^{7}G, m^7Gppppm^{7}G and GpppG) the observed K_{as} must be divided by two because of entropic effects. Only this normalized K_{as} represents a true microscopic association constant $K_{as}^{(micro)}$, reflecting the intrinsic stabilization energy of the complex. The macroscopic K_{as}, however, corresponds to the effective biological potency of the cap analogues.

Recently, the eIF4E–m^7GpppG binding affinity was fluorometrically studied in context of cell growth suppression by the promyelocytic leukemia protein.[41] The association constant resulting from these studies was $0.83(\pm 0.14) \times 10^6\ M^{-1}$ (23 °C, pH 7.5, 300 mM KCl). The K_{as} value determined by us for m^7GpppG is $7.39(\pm 0.46) \times 10^6\ M^{-1}$ (20 °C, pH 7.2, 100 mM KCl, Table 1) and $5.13(\pm 0.81) \times 10^6\ M^{-1}$ at elevated temperature (24.4 °C, pH 7.2, 100 mM KCl; Niedzwiecka, unpublished). According to the dependences discussed below, the pH-shift and especially electrostatic screening upon elevation of KCl concentration from 100 mM to 300 mM attenuate the eIF4E–m^7GpppG binding ~sixfold. Therefore, we would expect K_{as} in the range of 0.8 to $1 \times 10^6\ M^{-1}$ under the same experimental conditions as used by the Borden's group,[41] in an agreement with their results.

Table 1. Binding free energies ($\Delta G°$) and equilibrium association constants (K_{as}) for various eIF4E–cap analogue complexes, at 20 °C

Cap analogue	Murine eIF4E (28–217)		Human eIF4E	
	$\Delta G°$ (kcal/mol)	$K_{as} \times 10^{-6}$ (M^{-1})	$K_{as} \times 10^{-6}$ (M^{-1})	
m^7GTP	−10.779 ± 0.021	108.7 ± 4.0	97 ± 30[a]	1.17 ± 0.12[b]
m^7GDP	−9.804 ± 0.043	20.4 ± 1.5		
m^7GMP	−7.922 ± 0.048	0.806 ± 0.067		
m^7G	−4.91 ± 0.15	0.0046 ± 0.0012		
et^7GTP	−9.412 ± 0.048	10.41 ± 0.86		
bz^7GTP	−9.718 ± 0.014	17.59 ± 0.43		
p-Cl-bz^7GTP	−10.260 ± 0.050	44.6 ± 3.8		
$m_2^{2,7}GTP$	−10.013 ± 0.048	29.2 ± 2.4		
$m_3^{2,2,7}GTP$	−6.91 ± 0.33	0.143 ± 0.080		
$m^7Gppp2'OmG$	−9.262 ± 0.037	8.04 ± 0.51		
m^7GpppG	−9.213 ± 0.036	7.39 ± 0.46	9.6 ± 0.8[a]	0.69 ± 0.07[b]
m^7GpppA	−8.947 ± 0.065	4.68 ± 0.52		
m^7GpppC	−8.703 ± 0.096	3.08 ± 0.51	4.8 ± 0.4[a]	0.48 ± 0.05[b]
$m^7Gpppm^7G^{(micro)c}$	−8.431 ± 0.085	1.93 ± 0.28		
$m^7Gpppm^7G^{(macro)c}$		3.86 ± 0.56		
$m^7GppppG$	−10.746 ± 0.025	102.8 ± 4.4		
$m^7Gppppm^7G^{(micro)c}$	−9.887 ± 0.035	23.5 ± 1.4		
$m^7Gppppm^7G^{(macro)c}$		47.0 ± 2.7		
GTP	−5.808 ± 0.027	0.0214 ± 0.0010		
GDP	−4.950 ± 0.059	0.0049 ± 0.0005		
GMP	−3.09 ± 0.90	0.0002 ± 0.0003		
$GpppG^{(micro)c}$	−4.938 ± 0.049	0.0048 ± 0.0004		
$GpppG^{(macro)c}$		0.0095 ± 0.0007		

[a] Values for refolded full length human eIF4E.[19]
[b] Values for m^7G-affinity purified full length human eIF4E.[18]
[c] Microscopic and macroscopic association constants, see the text for details.

Binding affinity *versus* inhibitory properties of cap analogues

In the pioneering work of Carberry *et al.*,[14] the association constants of two fundamental cap analogues, m^7GTP and m^7GpppG, for eIF4E from human erythrocytes purified by cap-affinity chromatography were determined as $3.87 \times 10^5\ M^{-1}$ and $3.70 \times 10^5\ M^{-1}$, respectively (23 °C, pH 7.6, without KCl). Similar K_{as} values in the range of 10^5–$10^6\ M^{-1}$ were reported for recombinant human eIF4E purified by the same method.[15–18] In these studies also no essential difference in affinity between m^7GTP and m^7GpppG was observed. While the association constants reported here are at variance with these data, they are very close to those obtained in our earlier work on recombinant full length human eIF4E, which was also purified *via* refolding from inclusion bodies without any prior contact with cap[19] (Table 1). These K_{as} values are up to 500-fold higher than those reported previously. Furthermore, our data reveal large affinity differences among cap analogues possessing different functional groups. The affinities represented by our K_{as} values correspond well to the inhibitory properties of the cap analogues observed in a rabbit reticulocyte lysate (Figure 4). In a kinetic model developed for the *in vitro* translational system,[21,42,43] the inhibition constant (K_I) was determined as the overall dissociation constant of the cap analogue from the 48 S initiation complex. Results of both approaches, biophysical and biochemical, point out the significance of the same structural features of the cap responsible for specific recognition, e.g. the presence and type of N(7)-substituent of guanine, the negative charge density in the phosphate chain, and the N^2 amino group with at least one proton capable of forming a hydrogen bond. Interestingly, the observed values of K_I are ~100 times greater than those of $1/K_{as}$, for all cap analogues. This apparently larger

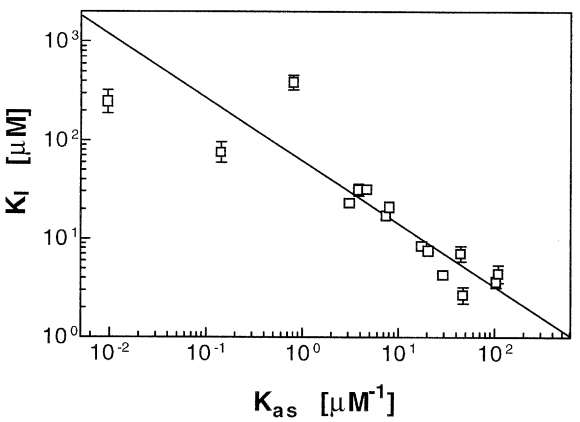

Figure 4. Correlation between inhibition constants K_I of the cap analogues obtained from *in vitro* translation (at 30 °C; data from Cai *et al.*[21]), and their fluorometrically measured equilibrium association constants K_{as} (at 20 °C; macroscopic K_{as} values were used for the symmetrical cap analogues, see the text). Correlation coefficient $r^2 = 0.795$.

amount of cap analogue required to inhibit translation *in vitro* than that necessary to displace eIF4E from the mRNA cap most likely arises from the following reasons. As opposed to HeLa cells,[44] the eIF4E concentration in reticulocyte lysate is not limiting for translation, and the majority of eIF4E is not engaged in this process.[45] The assumption underlying the determination of K_I values, that eIF4E concentration is negligible in comparison with that of a competitive inhibitor,[43] is not applicable here. The concentration of eIF4E is up to 50-fold higher than previously thought,[46] so much more than a 50-fold higher cap analogue concentration is required to inhibit translation due to the quadratic form of the equilibrium equation. Besides, protein synthesis results from a large number of catalytic reactions and depends not only on the eIF4E activity. In the *in vitro* experiments, the mRNA binding activity of eIF4F complex is enhanced by the presence of eIF4G.[47]

Parsing the free energy of binding: energetic cost of 7-substituent alteration

A comparison of standard Gibbs free energies of binding ($\Delta G°$) rather than that of association constants reflects the biophysical basis of the ligand affinity for the protein (Table 1). Contributions to $\Delta G°$ of single structural modifications of the cap are defined in Table 2. The presence of each type of substituent at the N(7) position of the guanine moiety produces a comparable effect on the eIF4E binding enhancement, in comparison with the non-substituted cap analogue, by $\Delta\Delta G°$ of -3.6 to -5 kcal/mol (1 cal = 4.184 J). The main gain of the stacking energy is reached irrespective of the nature of the substituent. This indicates that the resultant positive charge at 7-methylguanine and not N(7)-substitution itself is of primary importance, and the enhanced cation–π stacking is crucial for the binding. The only direct interaction involving the 7-methyl group is a nonspecific van der Waals contact with Trp166 in the complex with m^{7}GDP (3.93 Å, Figure 1(a)), which is lost in the complex with m^{7}GpppG (4.17 Å, Figure 1(b)). Replacement of the methyl group for larger substituent (ethyl, benzyl) can cause steric hindrance, and can interfere with creation of the water-mediated hydrogen bonds stabilizing the α-phosphate. Thus, it is energetically unfavourable by $\Delta\Delta G°$ of +0.5 to +1.4 kcal/mol.

Contributions of the phosphate groups

Data in Table 2 show a clear accordance of the $\Delta\Delta G°$ values related to the phosphate interactions between two series of compounds: 7-methylated and nonmethylated guanosine phosphates. Addition of the phosphate groups one after another is accompanied by formation of direct or water-mediated hydrogen bonds and salt bridges, yielding the same free energies in the two groups of compounds. This finding shows that there is no influence of the positive charge resulting from N(7)-methylation on the charge distribution at the phosphate chain. $\Delta\Delta G°$ for each step agrees with the number of intermolecular contacts revealed by

Table 2. Changes in the standard Gibbs free energy ($\Delta\Delta G°$) on eIF4E binding to the structurally modified cap analogues, at 20 °C

Structural alteration	($\Delta\Delta G°$ (kcal/mol))				
Replacement of N(7)-methyl for larger substituents: $\Delta\Delta G° = \Delta G°(x^7GTP) - \Delta G°(m^7GTP)$					
m → x:	m → et	m → bz	m → *p*-Cl-bz		
x^{7}GTP	+1.37 ± 0.05	+1.06 ± 0.03	+0.52 ± 0.05		
Methylation at N(7) for *n* phosphate groups: $\Delta\Delta G° = \Delta G°(m^7Gp_n(G)) - \Delta G°(Gp_n(G))$					
n:	1	2	3		
Gp$_n$ → m^{7}Gp$_n$	−4.83 ± 0.90	−4.85 ± 0.07	−4.97 ± 0.03		
Gp$_n$G[a] → m^{7}Gp$_n$G			−4.28 ± 0.06		
Addition or alteration of the second nucleoside: $\Delta\Delta G° = \Delta G°(m^7Gp_nY) - \Delta G°(m^7Gp_nX)$					
X → Y	none → G	G → m^{7}G[a]	G → A	G → C	G → 2′OmG
m^{7}Gp$_3$X → m^{7}Gp$_3$Y	+1.57 ± 0.04	+0.78 ± 0.09	+0.27 ± 0.07	+0.51 ± 0.10	−0.05 ± 0.05
m^{7}Gp$_4$X → m^{7}Gp$_4$Y		+0.86 ± 0.04			
Gp$_3$X → Gp$_3$Y[a]	+0.87 ± 0.06				
Successive addition of the 5′-phosphate groups: $\Delta\Delta G° = \Delta G°(n+1) - \Delta G°(n)$					
n → *n* + 1:	0 → 1	1 → 2	2 → 3	3 → 4	
m^{7}Gp$_n$	−3.01 ± 0.16	−1.88 ± 0.06	−0.98 ± 0.05		
Gp$_n$		−1.86 ± 0.90	−0.86 ± 0.07		
m^{7}Gp$_n$G				−1.53 ± 0.04	
m^{7}Gp$_n$m^{7}G[a]				−1.46 ± 0.09	
Successive addition of the N^2-methyl groups: $\Delta\Delta G° = \Delta G°(n+1) - \Delta G°(n)$					
n → *n* + 1:	0 → 1	1 → 2			
m$_n^{2,2}$m^{7}GTP	+0.77 ± 0.05	+3.10 ± 0.33			

[a] For symmetrical cap analogues $\Delta\Delta G°$ calculated from the microscopic association constant $K_{as}^{(micro)}$, see the text for details.

the crystallographic structures of the eIF4E–cap complexes (Figure 1). The α-phosphate forms a direct salt bridge with $N^{\zeta 2}$ of Arg157 as well as three indirect hydrogen bonds with $N^{\varepsilon 1}$ of Trp102, $N^{\varepsilon 1}$ of Trp166 and $N^{\zeta 2}$ of Arg112 *via* five water molecules trapped in the cavity of the binding centre. All water-mediated hydrogen bonds satisfy a requirement of tetraedral geometry of the water molecules and the P^{α}-oxygen anion. These five bridging water molecules support the same hydrogen-bonded network both in the eIF4E–m^7GDP complex[11] and the eIF4E–m^7GpppG complex, and are present also in the crystallographically independent second complexes in the asymmetric units. The total free energy of the α-phosphate stabilization is $\Delta\Delta G^\circ = -3.01(\pm 0.16)$ kcal/mol (Table 2). The β-phosphate group makes a salt bridge with N^{ζ} of Lys162 and a hydrogen bond with N^{ε} of Arg157, with total $\Delta\Delta G^\circ = -1.88(\pm 0.06)$ kcal/mol, i.e. about −0.94 kcal/mol per one direct bond. This indicates average $\Delta\Delta G^\circ$ of about −0.7 kcal/mol per one water-mediated hydrogen bond in case of the α-phosphate. The latter value is slightly less than the typical magnitudes of hydrogen bonds and salt bridges in a solvent accessible region in proteins ($-1.3(\pm 0.6)$ kcal/mol)[53,54] due to the entropic cost of ordering the water molecules. The γ-phosphate of m^7GpppG is stabilized by an additional, bifurcated salt bridge with N^{ζ} of Lys206 of a similar energy about −0.92 kcal/mol (Figure 1(b)).

Extension of the phosphate chain by the δ-moiety in the dinucleotide cap analogues gives an energetic gain of about −1.5 kcal/mol, what cancels out the energetic cost of the second guanosine addition to m^7GTP (Table 2). Most likely the δ-phosphate is additionally bound, and the entropic cost due to loss of some conformational degrees of freedom of the second nucleoside partially cancels the stabilization effect. However, it is also likely that the δ-phosphate does not interact directly with eIF4E, but the four-membered chain secures the necessary conformational freedom for the unbound second nucleoside, enabling the remaining m^7Gppp-part of the cap to bind more tightly. Thus, the presence of the δ-phosphate in m^7GppppG restores the affinity for the dinucleotide cap analogue ($\Delta G^\circ = -10.779(\pm 0.021)$ kcal/mol) to the same level as for m^7GTP ($\Delta G^\circ = -10.746(\pm 0.025)$ kcal/mol).

General separation of the binding free energy

The binding free energy of the 7-methylated analogues association with eIF4E appears to be totally separated into two groups of interactions: stacking together with hydrogen bonding and binding through the phosphate groups (Figure 1, Table 1). Irrespective of the level of the cap analogue phosphorylation, methylation at N(7) is accompanied by almost constant binding free energy change, $\Delta\Delta G^\circ$ about −4.9 kcal/mol (Table 2). Surprisingly, the measured values of ΔG° satisfy the relationship: $\Delta G^\circ(m^7Gp_n) = \Delta G^\circ(m^7G) + \Delta G^\circ(Gp_n)$, for $n = 1$, 2 or 3. This means that the 7-methylguanosine binding is separate from binding of the phosphate chain. The possible entropic cost arising from a change in the degrees of freedom due to linkage of the two moietes is either negligible or can be partially cancelled out if the bound phosphate groups facilitate to some extent penetration of the cap-binding slot by m^7G. The resultant effect is, however, below the best experimental accuracy: $\delta(\Delta G^\circ(m^7Gp_n) - \Delta G^\circ(m^7G) - \Delta G^\circ(Gp_n)) = \pm 0.16$ kcal/mol. The total binding free energy of 7-methylguanosine, $\Delta G^\circ(m^7G) = -4.91(\pm 0.15)$ kcal/mol (Table 1), is the same as $\Delta\Delta G^\circ$ resulting from methylation at N(7) (Table 2), which demonstrates that the ribose does not contribute to the complex stabilization. The 3D structures show only one nonspecific van der Waals contact between the ribose and Trp56 (Figure 1).

The stabilization energy of the GMP–eIF4E, GDP–eIF4E and GTP–eIF4E complexes originates only from the interactions involving the phosphate groups, independently pointing to the minute role of the ribose in stabilization of the complex. It is directly seen from the comparison of the total binding energy, $\Delta G^\circ(\text{GMP}) = -3.09(\pm 0.90)$ kcal/mol (Table 1), with the contribution of the single α-phosphate (Table 2). These findings reveal that although unmethylated guanosine phosphates are potentially capable of forming three Watson–Crick like hydrogen bonds, such bonds are not created. It is only when the guanine moiety is 7-substituted that the hydrogen bonds are formed. As shown above, the positive charge at m^7G determines the cap affinity for eIF4E being a cause of the stacking enhancement. Hence, the most striking conclusion is that the cation–π stacking enhancement is a precondition for the hydrogen bond formation, and a double role should be attributed to the presence of the conserved tryptophan residues 56 and 102 in the eIF4F binding site: stabilization of the 7-methylguanine ring by stacking itself and enabling 7-methylguanine to form the hydrogen bonds with the carboxylate oxygen atoms of Glu103 and the backbone amino group of Trp102 (Figure 1). Consequently, the system of m^7G–eIF4E works according to the "all-or-nothing" rule.

This mechanism elucidates why compounds containing unmethylated guanine moiety, potentially capable of forming three hydrogen bonds involving O^6, N(1) and N^2, do not competitively inhibit translation[21] and are unable to bind eIF4E as well as an other cap-binding protein, the mRNA 5′ cap-specific viral methyltransferase VP39.[49,50] Enhanced stacking of the methylated, positively charged bases with two parallel aromatic side chains of VP39 (Tyr22 and Phe180) plays a dominant role in the cap-recognition,[49] and hydrogen bonding is of secondary importance.[51] The structural requirements for the specific cap recognition were qualitatively examined by means of the fluorometric titration applied to GST-fused

eIF4E and His-tagged VP39, with the mutated cap-binding sites.[20] Although VP39 and eIF4E do not share a common phylogenetical ancestor, they use a similar mode of cap binding.

Energetic cost of the second nucleoside addition and modification

All of the dinucleoside triphosphates bind to eIF4E less strongly than m^7GTP, by $\Delta\Delta G°$ of +1.6 to +2.4 kcal/mol, and even with lesser strength than m^7GDP (Tables 1 and 2). The decreased affinity seems to suggest that the second nucleoside does not bind to eIF4E directly. Independently from the affinity studies, the same conclusion arises from the cocrystal structure of m^7GpppG bound to eIF4E. Figures 1(b) and 5 show the only part of m^7GpppG, which can be detected from the crystallographic data. The three phosphate groups are bound, while there is no defined electron density for the second guanosine. Hence, the m^7Gppp-part of the mRNA 5′ end is the crucial structural element for recognition by eIF4E.

The presence of the unbound fragment can destabilize the remaining intermolecular contacts of the cap. Addition of the second guanosine to GTP gives disadvantageous entropic effect by $\Delta\Delta G°$ of about +0.9 kcal/mol, while the second guanosine attached to m^7GTP results in $\Delta\Delta G°$ about +1.6 kcal/mol (Table 2). This larger value, together with our finding that GTP is bound only through the phosphate groups, indicates that the interactions of the 7-methylguanine moiety in m^7GpppG are also disturbed by the unbound second nucleoside "hanging" on the phosphate chain, by $\Delta\Delta G°$ of about +0.7 kcal/mol. Comparison of the cocrystal structures of eIF4E bound to m^7GDP and m^7GpppG shows clearly that two hydrogen bonds with Glu103 (donor–acceptor distances > 3 Å) and the van der Waals interaction of the 7-methyl group with Trp166 (distance > 4 Å) are indeed destabilized (Figure 1). Since only the m^7Gppp-part is responsible for stabilization of the m^7GpppG–eIF4E complex, ordering of the larger, dinucleotide molecule by means of the same but attenuated interatomic contacts as for the mononucleotide is energetically less favourable. Weaker binding of the dinucleotide, that resembles the natural capped mRNA better than m^7GTP, may seem contraintuitive. It should be stressed however, that there are three independent, experimetal proofs: the *in vitro* inhibition studies,[21] the current binding studies, and the X-ray data. These results confirm the suggestion that "clamping" by the putative phosphate bridge between Ser209 and Lys159 is needed to keep the longer mRNA chain tightly in place after 5′ cap–eIF4E binding.[52] Stronger affinity of the dinucleotide is by no means the obvious requirement.

Methylation of the second guanine at N(7) decreases the affinity of tri- and tetraphosphate dinucleotide caps to the same extent, $\Delta\Delta G°$ about +0.8 kcal/mol, consistent with attenuation of the negative charge of the phosphate chain (see below) and, at least partially, with the entropic cost of ordering the larger molecule. Exchange of the second base for adenine or cytosine is energetically less favourable. A minute advantageous effect in comparison with m^7GpppG appears after methylation of the second ribose at O(2′), which is however in the range of the experimental error.

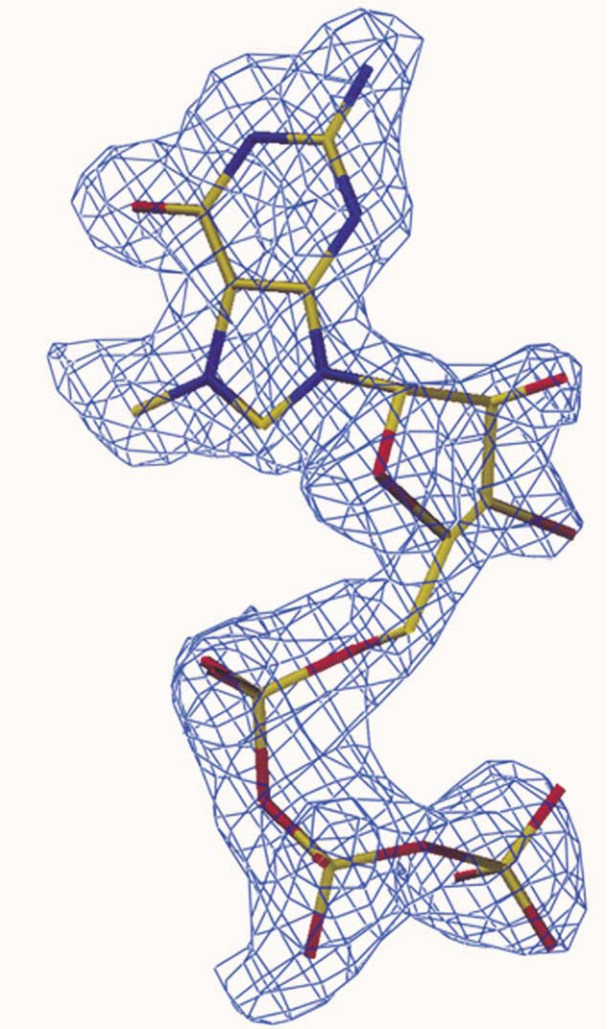

Figure 5. Experimental electron density map for m^7GpppG bound to murine eIF4E. The second nucleoside could not be detected by crystallography.

Energetic cost of methylation of the N(2)-amino group

Large $\Delta\Delta G°$ of +3.1 kcal/mol that accompanies substitution of the second amino-proton for the methyl group at N^2 of guanine, points to disruption of possibly more than one hydrogen bond between eIF4E and the cap. If one subtracts the steric and hydrophobic costs ($\Delta\Delta G°$ of about +0.8 kcal/mol, as observed for the methyl substitution of the first amino-proton, Table 2), the resulting energy (about +2.3 kcal/mol) suggests breaking of not only the Glu103–COO···HN^2–

m^{7}GTP hydrogen bond but also the second hydrogen bond, Glu103–COO···HN(1)–m^{7}GTP, most likely due to steric effects of the bulk dimethylamino group, which can move the acceptor group of Glu103 away.

Electrostatic effects and osmotic stress upon eIF4E–cap binding

The experimentally observed equilibrium binding constant depends on the environmental variables, i.e. ionic strength, osmolality, and the pH value of the solution.[55–57] In order to complete the ΔG° parsing, eIF4E–cap interaction had to be examined regarding the salt effects.[58] This has been performed in two complementary ways: according to (1) Davies-Stockes-Robinson electrostatic screening theory[59,60] and (2) stoichiometric Wyman linkage analysis.[61]

(1) At elevated KCl concentration the interaction is strongly attenuated (Figure 6). Screening by ionic strength (I) of the electrostatic attraction between eIF4E and the cap analogues of increasing negative charges, i.e. m^{7}GDP, m^{7}GpppG, m^{7}GTP and m^{7}GppppG, is qualitatively shown as a linear function of $I^{1/2}$ (Figure 6, inset), on the basis of the simple Debye–Hückel limited law ($a_j = 0$, $\Delta N = 0$). The negative slope of the regression line is approximately proportional to the charge at the phosphate chain, assuming that the terminal phosphate groups in the mononucleotide cap analogues are not fully ionized at pH 7.2 ($pK_a^{phosph} \sim 6.1$–6.5[62]). Monovalent cations were reported to significantly increase *in vitro* translation in rabbit reticulocyte lysate, and K$^+$ appeared to have the most suitable radius to support translation.[63] As the efficiency of eIF4E–mRNA 5′-cap binding decreases at higher K$^+$ concentration, the positive effect caused by K$^+$ should rather be attributed to the regulation of other translation components.

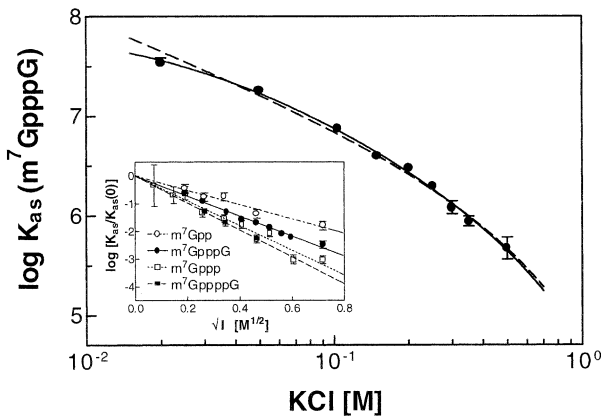

Figure 6. Determination of hydration number ΔN from KCl-dependence of the eIF4E–m^{7}GpppG complex formation, at 20 °C. Analysis according to electrostatic screening theory (continuous line) and stoichiometric cation release with the cation number $c = 1$ (broken line). Debye–Hückel analysis for four selected cap-analogues with increasing negative charges shown in the inset.

An extended analysis, including finite dimensions of the interacting molecular spheres and the hydration effects revealed by the osmotic stress, has been performed for m^{7}GpppG (Figure 6). The optimal result has been obtained within Davies approximation for the effective ionic diameter $a_j = 8$ Å, which describes the sum of the radii of the interacting species, i.e. three-membered phosphate chain of m^{7}GpppG and the group of four positively charged amino acid residues localised at the entry of the eIF4E cap-binding slot (Arg112, Arg157, Lys162 and Lys206, Figure 1). The product of mutually attracting charges is $z_1z_2 = -11.54 \pm 0.95$ e. Previous studies show that the resultant protein charge is only +0.58 e, while a dipole moment is substantial (579 D).[64] Hence, the cap recognizes directly the binding site of eIF4E and not the protein as a whole, and the charge localized on the guanine moiety does not by itself play any important role in the first step of the encounter. The negatively charged phosphate chain serves as a molecular anchor, enabling the cap to form further contacts within the binding site. These data provide us with the molecular interpretation of the free energy separation (Table 2), and the two-step mechanism observed for the cap–eIF4E association by means of stopped-flow spectroscopy.[64] The first step can be now attributed to the anchoring the phosphate group on the external basic amino acid residues, and the second step to the cooperative interactions deeply inside the m^{7}G-binding slot, i.e. cation–π stacking and hydrogen bonding with Trp56, Trp102 and Glu103. As all these residues are located at the flexible loops,[11] this second step of the complex formation is expected to involve a conformation change. The two-step model could be verified by mutant analysis, a mirror reflected methodological approach to the current cap analogue studies. The mutations eliminating all phosphate interactions should yield the equilibrium K_{as} for m^{7}GTP close to that for m^{7}G (Table 1) and considerably decrease the kinetic encounter rate constant k_{+1}. The complete cap-slot mutations should retain only the phosphate binding affinity, with K_{as} as for GTP and the k_{+1} unchanged. However, some mutations of crucial residues can change not only the nature of amino acid residues, but also the internal structure of the protein (local or even global fold), thus obscuring the investigated effect. By contrast, the studies based on the cap analogues, where each chemical alteration can be individually controlled, are free from such pitfalls.

The analysis of electrostatic screening confirms a biological role of a putative phosphate bridge connecting Ser209 with Lys159. It is thought to "clamp" the previously bound mRNA chain[52] when eIF4E is phosphorylated by the eIF4G-associated Mnk1 kinase.[65,66] As the phosphate chain of the cap is electrostatically steered toward the binding site, the mechanism of a "clamping cycle",

where the phosphorylation happens after the cap–eIF4E binding,[52] is most likely. Otherwise, if the phosphorylation at Ser209 occurred prior to the cap binding, it would attenuate the electrostatic attraction between eIF4E and the cap. Therefore, the affinity of the cap to the previously phosphorylated protein would be decreased. Recent data showing the effect of eIF4E phosphorylation on cap–eIF4E affinity[67] support this conclusion.

Molecular crowding of the solution causes a shortage of the free water molecules. The K_{as} at elevated salt concentration decreases more than it could be explained by electrostatic screening only, indicating that the binding of the cap to eIF4E requires additional hydration of the molecular surfaces. It should be noted that, although the activity of water at the maximal salt-concentration in the present study was not very far from unity ($a_w \sim 0.97$ at 0.5 M KCl), the hydration effects appear quite distinctly, and the considerable number of water molecules that are taken up to the cap–eIF4E complex has been detected: $\Delta N = 68 \pm 16$.

The association constant of m^7GpppG extrapolated to the optimal conditions, i.e. without electrostatic screening and osmotic stress, is $K_{as}(0) = 1.12(\pm 0.18) \times 10^9\ M^{-1}$. It is 150-fold greater than K_{as} measured in 100 mM KCl, and is an evidence of the strong electrostatic contribution to eIF4E–cap binding. On the other hand, the association constant extrapolated to the pseudostandard state of 1 M KCl is $K_{as}(1) = 4.8(\pm 1.9) \times 10^4\ M^{-1}$. In spite of strong electrostatic screening, the intrinsic thermodynamic preference of eIF4E for the methylated cap is still efficient. This completely screened interaction of eIF4E with m^7GpppG at 1 M KCl has exactly the same association constant as m^7G, the analogue insensitive toward electrostatic interactions, $K_{as}(m^7G) = 4.6(\pm 1.2) \times 10^4\ M^{-1}$ (Table 1). Hence, at ionic strength of 1 M all the interactions with the phosphate groups are lost.

(2) In terms of Wyman linkage analysis, stoichiometrical ionic interactions are taken into account in the same manner as excluded volume effects. In our case, the most probable processes accompanying eIF4E–cap binding are cation (K^+) release from the phosphate chain of the cap analogue and a change of preferential hydration:

$$\text{cap}\bullet(cK^+) + \text{eIF4E} + \Delta N H_2O \rightleftarrows \text{cap}\bullet\text{eIF4E}\bullet(\Delta N H_2O) + cK^+$$

where c is the number of K^+ released from the ligand, $c = 0.826 \pm 0.092$ (Figure 6), indicating that possibly one K^+ is displaced from the phosphate chain of m^7GpppG upon binding to eIF4E. Cation release (polyelectrolyte effect) was extensively studied for the entropy-driven *B*-DNA interactions with oligocations[55] Large contribution of the counterions displacement into bulk solvent was also reported for anthracycline antibiotic binding to DNA.[8] Because the cap analogues lacked substantial axial charge distribution, such as that observed in the helical *B*-DNA polyanion, the cation dilution effect is much less pronounced. The contribution of the electrolyte effect to the stability of the m^7GpppG–eIF4E complex at 100 mM KCl is $\Delta G^\circ_{el} = -1.53(\pm 0.15)$ kcal/mol, in comparison with the total free energy of m^7GpppG binding upon these conditions, $\Delta G^\circ = -9.213(\pm 0.036)$ kcal/mol (Table 1), so the entropic contribution to the association driving force, resulting from the cation release, is rather moderate. The association constant calculated from the stoichiometrical model and extrapolated to 1 M KCl is the same as that derived from the approach of the continuous screening, $K_{as}(1) = 4.45(\pm 0.34) \times 10^4\ M^{-1}$. Relatively high $K_{as} \sim 10^4$ of m^7GpppG at 1 M KCl distinguishes our cap–eIF4E system from the counterion release-driven DNA–oligocation system, for which the corresponding value was within an order of magnitude with unity.[55]

The number of water molecules that have to be taken up is $\Delta N = 95 \pm 18$. Keeping the constant value of $c = 1$ does not cause significant worsening of the fit, according to the Snedecor's *F*-test ($P = 0.11$), and gives $\Delta N = 63.5 \pm 9.3$. Both of these values agree within the numerical accuracy with ΔN derived from the complementary model of electrostatic screening, so the two theoretical treatments indicate the same extent of water participation in the cap binding event. In respect of the direct interaction with the electrolyte, the Snedecor's *F*-test determines that the screening theory is better ($R^2 = 0.9967$) than the cation release approach ($R^2 = 0.9906$ for $c = 1$), on the significance level of $P = 0.0155$. Hence, the description in terms of continuous screening by the ionic atmosphere of the excess salt is more relevant. The possible stoichiometric interaction with the counterion contributes to the screening, and additionally provides the advantageous entropic effect to the binding.

Significance of the electrostatic forces in kinetics of the eIF4E–cap complex formation was also shown by the fluorescence stopped-flow measurements.[64] The association rate constant k_{+1}, measured experimentally and confirmed by Brownian dynamics simulations, was markedly diminished by the ionic strength, while the dissociation rate constant k_{-1} was slightly increased. However, the estimated rate constants k_{+2} and k_{-2} of the internal rearrangement of the initial complex were also ionic strength-dependent and this could not be explained when neglecting the excluded volume effects. Now, in light of the osmotic stress analysis, we can explain the decrease of the second-step rate constant k_{+2} and the increase of k_{-2} in terms of the conformational change, upon which the significant number of water molecules have to hydrate the protein surface.

For several years increasing attention was paid both to hydration changes and ion exchange that can accompany ligand binding by the proteins that show simultaneous conformational

changes,[56,68–70] e.g. the hydration of hemoglobin by 60–65 water molecules and the release of one chlorine anion occur with the transition from the deoxy T to fully oxygenated R state.[57] Recently, it was shown that DNA binding of various intercalators was accompanied by the uptake of 0–30 water molecules.[71] On the other hand, the entropy-driven association of lac repressor to lac operator DNA is accompanied by the release of ~200 water molecules.[72] In our cap–eIF4E system, the additional hydration is similar to that for the hemoglobin oxygenation. The number of water molecules (~65) taken up from the bulk solvent is much greater than that inside the cap-binding centre, found by crystallography (9 and 16, in the complex with m^7GDP[11] and m^7GpppG, respectively), and refers to changes in the first-layer hydration shell of the molecular surfaces.[73] Such extensive hydration of eIF4E would respond to exposure of additional ~450 Å^2 of the molecular surface area to contact with water.[57,69] It is consistent with other evidences of a substantial conformational change of eIF4E, i.e. the rearrangement of the encounter complex,[64] the profound (~65%) quenching of the intrinsic fluorescence of eIF4E upon cap binding, significantly different fluorescence quenching patterns when comparing interactions of apo-eIF4E and cap-saturated eIF4E with the 4E-BP1 and eIF4G peptides (see below, Figure 9, Table 3), and deaggregation of eIF4E (residues 33–217) forced by the cap analogues binding (Dynamic Light Scattering data; Niedzwiecka, unpublished).

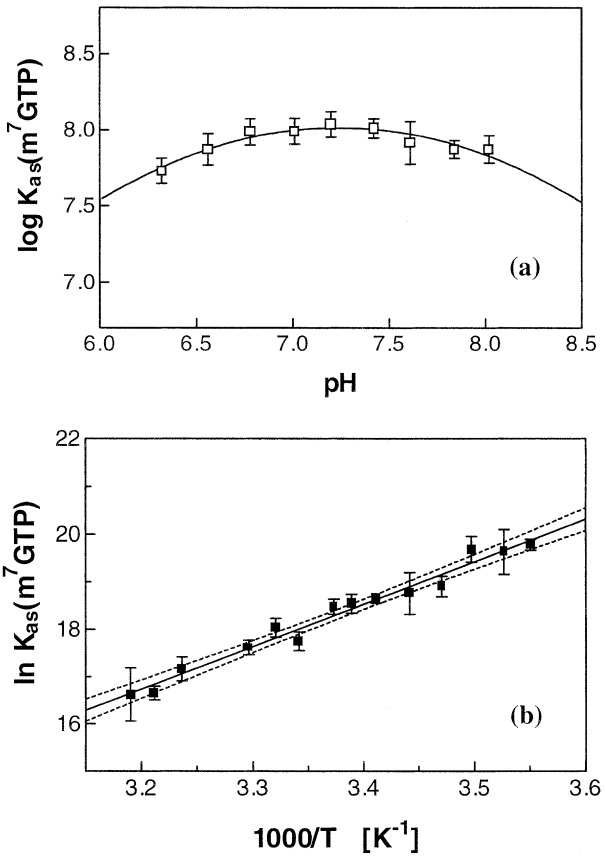

Figure 7. (a) Binding of m^7GTP to eIF4E as a function of pH, at 20 °C. (b) van't Hoff plot for eIF4E–m^7GTP complex formation, at pH 7.2. The dashed lines indicate 95% confidence interval of the regression line.

Ionic equilibria in eIF4E–cap complex

7-Methylguanosine is a mixture of positively charged and zwitterionic forms due to dissociation of N(1)–H (pK_a, ~7.24–7.54[48]). The pK_a drop by ~2 units upon 7-substitution of guanosine was suspected to have a biological significance, and the zwitterionic form was initially postulated to be responsible for interaction with eIF4E.[14,74] In contrast, structural data indicated that the cationic form of m^7GDP binds to eIF4E, because of the spatial distances suitable for a hydrogen bond between Glu103 and N(1)–H (PDB accession no: 1EJ1, 1AP8).[11,12,29] However, the N(1)–H proton was not directly observed during the NMR experiment,[12] so the issue is still not entirely resolved.

In the present study, the affinity of eIF4E for m^7GTP as a function of pH (Figure 7(a)) has the optimum at pH 7.24 ± 0.13, close to the physiological pH of 7.4, and lower than pH 7.6 reported for the full length eIF4E purified by m^7G-affinity chromatography.[14] The pH-dependence of K_{as} is rather flat, providing a wide pH-range of efficient cap–eIF4E binding. From the Wyman model,[61] two effective acidic dissociation constants have been determined: pK_L = 7.99 ± 0.14 for N(1)–H of the cap in the presence of eIF4E, and pK_p = 6.49 ± 0.13 for the hydroxyl group of Glu103 in the presence of the cap (the errors are numerical; the real accuracy is closer to 1 pK unit due to simplicity of the model). The elevated effective pK_L shows that m^7G exists in a cationic form in the eIF4E-bound state and donates N(1)–H proton for the hydrogen bond with the deprotonated carboxyl group of Glu103, what is consistent with the structural data. Hence, the decrease of pK_L upon 7-methylation is partially cancelled by the protein microenvironment. The entirely different affinity of the 7-methylated nucleotides *versus* their unmethylated counterparts results from different stacking ability (see above), and does not arise from different acidic/basic properties as was suggested previously.[14,74]

Thermodynamics

The temperature dependence of association constant for m^7GTP (Figure 7(b)) provides the thermodynamic parameters of the binding. The strong specific interaction between eIF4E and m^7GTP is unambiguously connected with a high enthalpy of association, $\Delta H^\circ = -17.76(\pm 0.86)$ kcal/mol. The binding is entropy-opposed with the resultant $\Delta S^\circ = -23.6(\pm 2.9)$ cal/mol K, in spite of the conducive entropic contribution resulting from

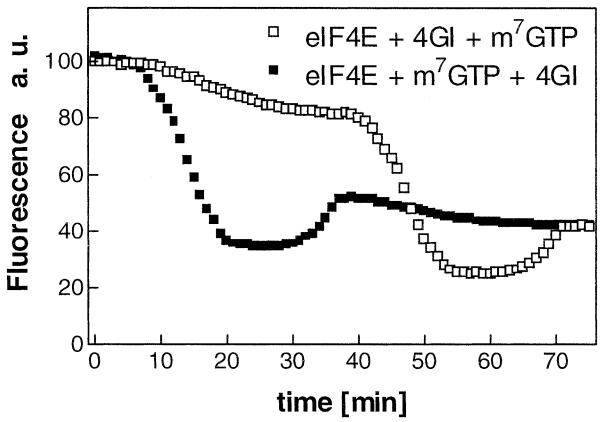

Figure 8. A typical time-course of fluorescence intensity for cross-titration experiment. Ternary cap–eIF4E–peptide complexes were formed *via* TST of apo-eIF4E (i) with the peptide and next with the cap (□; 0–5 minutes, initial baseline; 6–38 minutes, titration with eIF4GI peptide; 39 minutes, intermediate baseline; 40–71 minutes, titration with m^{7}GTP; 72–76 minutes, final baseline), and (ii) in the reverse sequence, with the cap and next with the peptide (■; 0–5 minutes, initial baseline; 6–37 minutes, titration with m^{7}GTP; 38 minutes, intermediate baseline; 39–71 minutes, titration with eIF4GI peptide; 72–76 minutes, final baseline). Measurements were performed in Hepes/KOH (pH 7.2), 100 mM KCl, 1 mM DTT, 0.5 mM EDTA, at 20 °C. Aliquots (1 μl) of increasing concentrations (1 μM to 5 mM) of the ligands were added to 1400 μl of eIF4E solution. Quenching was monitored at 355 nm, for the excitation wavelength of 290 nm, what ensured elimination of tyrosine fluorescence. The fluorescence intensity was corrected for the dilution and the inner filter effect. The corresponding titration curves (concentration dependences) are shown in Figure 9.

displacement of one K^+ from the three-membered phosphate chain. Such contribution for m^{7}GTP is expected to be not less than that for m^{7}GpppG, $\Delta S°_{el} = +5.22(\pm 0.51)$ cal/mol K, due to the presence of an additional possible K^+-binding site at the unblocked edge of the mononucleotide cap analogue. Examination of the van't Hoff plots for interactions between eIF4E and other mono- and dinucleotide cap-analogues shows that they are also mainly enthalpy-driven in the range of studied temperatures (Niedzwiecka, unpublished results).

Cooperativity in ternary peptide–eIF4E–cap complexes

Binding of the eIF4GI, eIF4GII or 4E-BP1 peptides to the convex dorsal surface of eIF4E leads to quenching of the protein intrinsic fluorescence, primarily due to interaction between Trp73 of eIF4E and three amino acid side chains of the peptides.[29] To check whether cap-binding and 4E-BP/eIF4G-binding are cooperative, we have performed cross-titration experiments with each peptide (Figure 8). Irrespective of the succession of the cap and the peptide added, the total final quenching after saturation of both eIF4E-binding sites is always identical. However, the partial quenching (Q) of the total initial fluorescence signal, which corresponds to saturation of one of the eIF4E binding sites, with and without the prior saturation of the other, is different (Figure 9, Table 3). The fluorescence quenching upon titration with m^{7}GTP of the peptide-saturated eIF4E is $<60\%$, while the apo-protein reveals $\sim 65\%$ of quenching. The quenching resulting from the peptide binding is $\sim 12\%$ for m^{7}GTP-saturated eIF4E and $\sim 19\%$ for the apo-protein. The differences between Q(apo) and Q(sat) are $\sim 3\%$ for the unphosphorylated 4E-BP1 peptide, $\sim 9\%$ for the phosphorylated 4E-BP1 peptides and $\sim 7\%$ for eIF4G peptides. This succession- and structure-dependent behaviour of the quenching patterns supports our previous conclusions pointing to the conformational change of eIF4E upon cap binding, and a possible conformational change upon the peptide binding.

The fluorometrically determined values of the association constants have been used to address the cooperativity problem by a direct quantitative comparison. All the eIF4E–peptide K_{as} are in the order of 10^7 M^{-1} (Table 3). The K_{as} values for binding of cap-saturated eIF4E to eIF4GI and eIF4GII

Table 3. Equilibrium association constants (K_{as}) and partial quenching (Q) of total initial fluorescence upon formation of the binary complexes of the apo-form of eIF4E with the eIF4GI, eIF4GII and 4E-BP1 peptides, and the ternary complexes (m^{7}GTP–eIF4E–peptide) of previously m^{7}GTP- or peptide-saturated eIF4E, at 20 °C. For reference the association constant of m^{7}GTP to eIF4E $K_{as} = 108.7(\pm 4.0) \times 10^6$ M^{-1} (see Table 1), $Q \sim 65\%$

	eIF4GI	eIF4GII	4E-BP1	4E-BP1 (P-Ser65)	4E-BP1 (P-Ser65/Thr70)
	$K_{as} \times 10^{-6}$ (M^{-1}) for the peptides				
eIF4E(m^{7}GTP-saturated)	21.43 ± 2.15	5.35 ± 0.20	9.47 ± 0.39[a]	4.77 ± 0.40[a]	5.72 ± 0.35[a]
eIF4E(apo)	13.65 ± 0.86	6.51 ± 0.19	10.59 ± 0.84	5.91 ± 0.44	5.74 ± 0.34
	$K_{as} \times 10^{-6}$ (M^{-1}) for m^{7}GTP				
eIF4E(peptide-saturated)	120.5 ± 7.2	137.9 ± 15.8	101.6 ± 7.3	107.4 ± 5.2	101.0 ± 8.6
	Fluorescence quenching Q (% of total initial fluorescence)				
eIF4E(m^{7}GTP-saturated)	12.1 ± 0.9	13.6 ± 2.1	15.1 ± 3.6	10.2 ± 5.5	11.3 ± 4.6
eIF4E(apo)	18.3 ± 1.2	20.6 ± 2.5	18.2 ± 9.5	18.8 ± 9.0	20.2 ± 1.4

[a] Data from Gingras *et al.*[31]

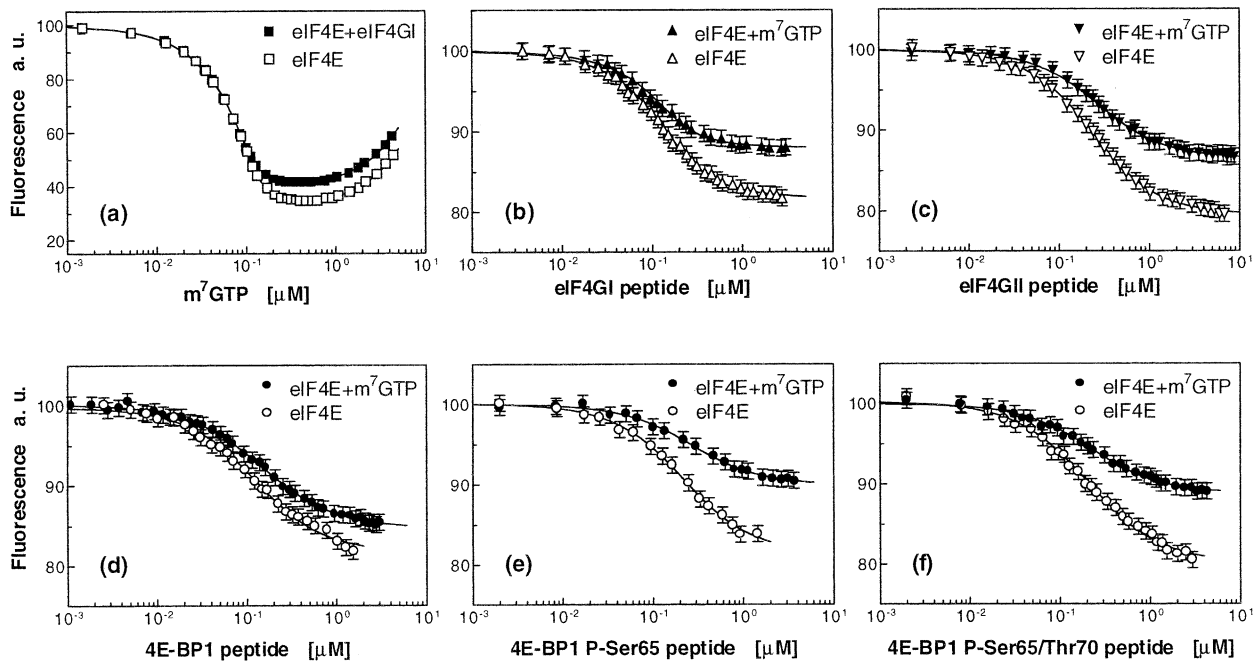

Figure 9. Comparison of the titration curves for formation or eIF4E binary and ternary complexes with m^{7}GTP and various BXX**YDR**X**FL**Φ oligopeptides. Titration of (a) apo-eIF4E with m^{7}GTP (□), and eIF4E–eIF4GI peptide complex with m^{7}GTP (■); (b) apo-eIF4E with eIF4GI peptide (△), and eIF4E-m^{7}GTP complex with eIF4GI peptide (▲); (c) apo-eIF4E with eIF4GII peptide (▽), and eIF4E–m^{7}GTP complex with eIF4GII peptide (▼); (d) apo-eIF4E with 4E-BP1 peptide (○), and eIF4E–m^{7}GTP complex with 4E-BP1 peptide (●); (e) apo-eIF4E with 4E-BP1(P-Ser65) peptide (○), and eIF4E–m^{7}GTP complex with 4E-BP1(P-Ser65) peptide (●); (f) apo-eIF4E with 4E-BP1(P-Ser65/Thr70) peptide (○), and eIF4E–m^{7}GTP complex with 4E-BP1(P-Ser65/Thr70) peptide (●).

peptides ($21.43 \times 10^6\ M^{-1}$ and $5.35 \times 10^6\ M^{-1}$, respectively) are close to those derived by isothermal titration calorimetry (ITC) ($37 \times 10^6\ M^{-1}$ and $6.7 \times 10^6\ M^{-1}$, respectively).[29] The peptide which bound the tightest to eIF4E is eIF4GI and its interaction is few but unambigously influenced by the apo- or cap-saturated state of eIF4E (Table 3), i.e. an 1.6-fold increase of K_{as} has been observed for the eIF4GI peptide binding to cap-saturated eIF4E. A similar effect, albeit to a lesser extent, appears also for the eIF4GII peptide. Reversely, a slight enhancement of the m^{7}GTP-affinity (only up to 1.3-fold, but quantitatively beyond experimental error) has been noted after previous saturation of eIF4E with eIF4GI or eIF4GII peptides (Table 3).

The eIF4G protein strongly enhanced the cross-linking effectivity of eIF4E to the mRNA 5′-cap structure.[47] On the other hand, our preliminary fluorescence study suggested no significant changes of the association constant for binding of eIF4E with the cap analogue in the presence of a 17-amino acid mammalian eIF4GII peptide.[75] Comparison of the crystallography-determined structures of binary and ternary complexes revealed also no important structural differences directly in the eIF4E-cap binding slot in the absence or presence of either the eIF4GII or 4E-BP1 peptide.[11,29] However, among nine crystallographically independent structures of the m^{7}GDP–eIF4E binary[11] and ternary[29] complexes, and the m^{7}GpppG complex, there are two cases where the C-terminal loop (206–213) located in the vicinity of the cap-binding site has fully ordered backbone, and the N terminus (28–35) close to the eIF4G/4E-BP binding site is concurrently ordered. In remaining cases both the loop and the N tail are unordered. These could indirectly suggest a possibility of cooperation between the two distant binding sites. Recently, it was shown by the gel-shift experiments and m^{7}GTP–Sepharose binding that a 17-mer fragment of yeast eIF4GI exerted a negligible influence on the eIF4E–cap interaction, but complete eIF4GI and larger fragments produced enhancement of the eIF4E–cap binding.[38] Finally, the quantitative results reported herein confirm that the putative cooperativity is possible (Table 3) but the minimal eIF4E-binding motif of eIF4G alone can be insufficient to induce changes evident in the crystal structure of the cap-binding site.[29]

In the case of 4E-BP1 peptides, the affinity for the apo-protein is the same as that for the cap-saturated eIF4E[31]. The K_{as} values for the unphosphorylated 17-mer peptide 4E-BP1 ($9.47 \times 10^6\ M^{-1}$,[31] and $10.59 \times 10^6\ M^{-1}$, present study) agree well with K_{as} calculated from ITC ($20 \times 10^6\ M^{-1}$).[29] ITC for the full length 4E-BP1 yielded higher K_{as} ($67 \times 10^6\ M^{-1}$). In terms of the binding free energy, however, this difference between $\Delta G°$ for the full length protein (−10.50 kcal/mol) and the peptide (−9.36 kcal/

mol) is small, what indicates that majority of the intermolecular contacts required for stabilization of the 4E-BP1–eIF4E complex are accomplished in the model system with participation of the short peptide.

Binding of full length 4E-BP1 and 4E-BP2 to eIF4E was reported to enhance the cap–eIF4E association, as suggested from m^7GTP-affinity chromatography and surface plasmon resonance (SPR).[36] The reversed cooperativity, i.e. an increase of the 4E-BP2 affinity for the cap-saturated eIF4E in comparison with apo-eIF4E was also found using SPR.[76] The differences in the fluorescence quenching patterns upon formation of the ternary complexes (Figure 9, Table 3), and arguments discussed above for the eIF4G peptides, point to a putative cooperation between the two binding sites. However, the binary 4E-BP1 peptide–eIF4E and cap–eIF4E interactions do not affect the association constants values for the further formation of the ternary peptide–eIF4E–cap complexes, within experimental errors (Table 3). No measurable affinity changes for the 17-mer and 25-mer fragments of 4E-BP1 could reflect the inability of the peptides to completely mimick the influence of full length 4E-BP1 on eIF4E.

Regulation of 4E-BP1 activity by phosphorylation

Phosphorylation of specific serine and threonine residues of 4E-binding proteins modulates their affinity for eIF4E.[52] A two-step mechanism of 4E-BP1 phosphorylation was proposed, involving phosphorylation on Thr37 and Thr46 as a priming event for subsequent phosphorylation of Ser65 and Thr70.[30] Recently Gingras *et al.*[31] showed *via* phosphopeptide mapping and fluorescence measurements of cap-saturated eIF4E, that both of these phosphorylation events were insufficient to disrupt the 4E-BP1 binding with eIF4E, and thoroughly discussed the possible sources of disagreement with the previous publications.[32–34] The present fluorescence quenching experiments for cap-free eIF4E confirm the results for the cap-saturated protein[30,31] (Table 3). The monophosphorylation of the 4E-BP1 peptide at Ser65 causes only ~2-fold decrease in the affinity for eIF4E ($\Delta\Delta G^\circ$ less than +0.4 kcal/mol), and diphosphorylation at both Ser65/Thr70 does not reduce the affinity further. Mono- and diphosphorylated 4E-BP1 peptides still retain the high ability to interact with eIF4E, with K_{as} about $5 \times 10^6\ M^{-1}$ and ΔG° about −9.0 kcal/mol. Thus, phosphorylation of both Ser65 and Thr70 is insufficient to abolish the eIF4E binding.

However, several authors reported substantial reduction of the eIF4E association with 4E-BP1 phosphorylated at Ser65 *in vitro*.[32–34] A nearly two orders of magnitude decrease of K_{as} was observed by means of SPR due to phosphorylation at Ser65 of the full length 4E-BP1 mutant in which alanine had been substituted at four Thr/Ser-P sites, leaving Ser65 susceptible to phosphorylation.[33] A value of K_{as} for the unphosphorylated mutant was determined as $278 \times 10^6\ M^{-1}$. ITC yielded a lower K_{as} value of $67 \times 10^6\ M^{-1}$ for the full length 4E-BP1,[29] but at this level of the equilibrium constants (corresponding to ΔG° about −11 kcal/mol) the 4-fold difference between K_{as} is not very significant ($\Delta\Delta G^\circ$ about 0.8 kcal/mol). Even taking into account the 75-fold drop of the association constant to $3.7 \times 10^6\ M^{-1}$ upon phosphorylation at Ser65 according to the SPR results,[33] the corresponding energy difference $\Delta\Delta G^\circ$ would be about +2.5 kcal/mol, which is not much in comparison with the remaining binding free energy of the monophosphorylated protein (ΔG° about −8.8 kcal/mol). Although the peptides seem not to be the perfect mimetic models for all properties of the full length protein, in light of the previous studies demonstrating that full-length 4E-BP1 monophosphorylated on Ser65 could bind to eIF4E efficiently, while no binding could be detected for 4E-BP1 deleted in the eIF4E-binding site,[31] the peptides are good models for investigations how single phosphorylation modulates the intermolecular interactions. The main conclusion which could be drawn from SPR[33] is the same as those from our fluorescence binding studies and phosphopeptide mapping,[31] that 4E-BP1 monophosphorylated at Ser65 still possesses the high, submicromolar affinity for eIF4E. Thus, phosphorylation of additional residues, most likely the priming sites Thr37 and Thr46, is required to release 4E-BP1 from eIF4E.[30]

Conclusions

Application of the exact quantitative approach to study eIF4E–cap interactions enabled us to explain hitherto unresolved issues. Parsing the binding free energy into the contributions of various structural elements of the cap points out their individual role in the two-step process of eIF4E–cap recognition. The 5′-phosphate chain is the primary anchor to eIF4E. The eIF4E–cap binding is accomplished by the specific contacts of three phosphate groups and m^7G moiety but not of the second nucleoside. The biological importance of methylation of guanosine at N(7) has been elucidated by showing that the thermodynamic origin of the strong discrimination between 7-methylated and unmethylated counterparts (5000-fold difference in K_{as}) consists in absolute cooperativity of cation–π stacking and hydrogen bonding, i.e. the enhanced stacking between the cationic m^7G and the aromatic Trp side-chains is necessary to stabilize effectively the base moiety, what is a precondition for formation of three hydrogen bonds inside the cap-binding slot. eIF4E selects precisely between the 7-monomethylguanine and 2,2,7-trimethylguanine analogues (760-fold difference in K_{as}). The temperature-dependence of K_{as} reveals enthalpic character of the binding and together

with the ionic strength-dependence emphasizes significance of electrostatic interactions for cap–eIF4E recognition. We have also checked possibilities of cation release and water exchange that can accompany the binding. The estimated water uptake to the hydration shell is relevant to conformational rearrangement of entire eIF4E upon the cap binding.

Comparison of the eIF4E-binding affinity of natural *versus* structurally modified cap analogues, together with the structures of the eIF4E–cap complexes, makes a solid foundation to rational design of new cap analogues with better inhibitory properties than those synthesized hitherto. This is a subject of pharmacological importance because of evidence implicating eIF4E and its regulatory 4E-BP proteins in malignancy and apoptosis.[22] Experiments with use of the short peptides suggest that cooperativity between cap and eIF4G/4E-BP-binding sites is possible. Phosphorylation of both Ser65 and Thr70 of 4E-BP1 has been proved insufficient to abrogate 4E-BP1 binding with apo-eIF4E, similarly as with cap-saturated eIF4E,[31] so additional phosphorylation of the priming sites Thr37 and Thr46 is necessary. Taken together, these results provide more profound insights into how eIF4E interacts with other components of the cytoplasmic machinery responsible for cap-dependent translation initiation.

Materials and Methods

Chemical syntheses and sample preparations

Syntheses and purification of the cap analogues were performed as described previously.[77–81] The cap analogue concentrations were obtained from weighted amounts (±5%). The cap analogues in solution at elevated pH (>8) undergo opening of the five-membered ring of 7-substituted guanine, followed by hydrolysis of the glycosidic bond.[82] As checked by NMR (Stolarski, unpublished) the cap was very stable at pH 7.2, and stable enough to perform fast experiments at higher pH.

Murine eukaryotic initiation factor eIF4E (residues 28–217) was expressed in *Escherichia coli*.[83] The protein was purified from inclusion bodies pellet and refolded by one step dialysis from 6 M guanidinum hydrochloride, followed by cation-exchange chromatography on a MonoS column, with a final yield up to 30 mg from 1 l of culture. The main goal of using refolded eIF4E was to avoid contact with cap analogues at any stage of purification, first of all the elution of the soluble fraction protein from the cap-affinity column by a cap analogue. Immediately before the spectroscopic measurements the protein sample was filtered through Millipore Ultrafree–0.5 ml Biomax 100 kDa NMWL. Total concentration of eIF4E was determined from absorption ($\varepsilon_{280} = 53{,}900\ cm^{-1}M^{-1}$).

Peptides corresponding to residues 569–580 of mammalian eIF4GI: KKRYDREFLLGF,[9] residues 621–637 of mammalian eIF4GII: KKQYDREFLLDFQFMPA,[10] and residues 51–67 of mammalian 4E-BP1: RIIYDRKFLMECRNSPV[27] were synthesized by Boc protocols for solid phase peptide synthesis and cleaved using a standard HF procedure.[84] Syntheses of a mammalian phosphopeptide P-Ser65 51–67 4E-BP1 and a diphosphopeptide P-Ser65/Thr70 51–75 4E-BP1 RIIYDRKFLMECRNSpPVTKTpPPKDL[27] was performed manually on a Wang resin (Novabiochem) using Fmoc protocols for solid phase phosphopeptide synthesis. Phosphoserine and phosphothreonine were directly incorporated during the synthesis as the corresponding preformed mono-protected *N*-α-Fmoc-*O*-benzyl phosphoaminoacid derivatives, purchased from Novabiochem.[85] The phosphopeptides were cleaved using trifluoroacetic acid/triisopropylsilane/water mixture (TFA/TIS/H_2O, 95:2.5:2.5). After cleavage, crude peptides were purified to homogeneity by semi-preparative HPLC, and characterized by amino acid analysis (see below) and MALDI-TOF or ESI spectrometry (569–580 eIF4GI peptide, predicted mass 1697.0 Da, measured mass 1698.0 Da; 621–637 eIF4GII peptide, predicted mass 2177.8 Da, measured mass 2178.0 Da; 51–67 4E-BPl peptide, predicted mass 2141.8 measured mass 2141; phosphopeptide, P-Ser65 51–67 4E-BP1, predicted mass 2220.1, measured mass 2221.0; diphosphopeptide, P-Ser65/Thr70 51–75 4E-BPI, predicted mass 3180.55, measured mass 3181.0). Concentrations of the peptides were determined after acid gas-phase hydrolysis and three independent amino acid analysis repeats. The amino acid residues were converted to phenylthiocarbamyl derivatives and separated on PicoTag 3.9 × 150 mm column (Waters, Millipore Co., U.S.A.) using Waters HPLC system, according to standard protocols. Solutions of 4E-BPI peptides were strictly controlled for lack of disulfide dimer formation. Dimers occured in the stock solution unless it was incubated at very high concentration of the reducing agent (13 mM DTT) at pH 7.5 for several days. This secured satisfactory monomerization, as rigorously checked on HPLC and MS. Then, the affinity measurements could be performed properly with use of more dilute peptide solution at 1 mM DTT. The problem concerned the phosphorylated 4E-BP1 peptides to lesser extent, since the presence of the negatively charged phosphate groups at Ser65 in the vincinity of Cys62 prevents the dimerization.

Spectroscopic measurements

The titration experiments were performed in a standard buffer: 50 mM Hepes/KOH (pH 7.20), 100 mM KCl, 1 mM dithiothreitol (DTT) and 0.5 mM disodium ethylenediaminetetraacetate (EDTA), except for the experiments at variable pH and ionic strength. pH (±0.01 unit) was measured independently at each temperature and ionic strength (Beckman Φ300 pH-meter, Germany). Absorption and fluorescence spectra were recorded on Lambda 20 UV/Vis and LS-50B instruments (Perkin–Elmer Co., Norwalk, CT, USA), in a quartz semi-micro cuvette (Hellma, Germany) with optical lengths 4 mm and 10 mm for absorption and emission, respectively. The sample was thermostated and the temperature was controlled with a thermocouple inside the cuvette (±0.2 °C). For eIF4E–cap association, the excitation wavelength of 280 nm (slit 2.5 nm, auto cut-off filter), and the emission wavelength of 335, 336 or 337 nm (slit 2.5–4 nm, 290 nm cut-off filter) were applied, with a correction for the photomultiplier sensitivity. For eIF4E–peptide binding, the excitation wavelength of 290 nm and the emission wavelength of 350 or 355 nm were used. These conditions ensured observation of the protein tryptophan residue emission, only. The fluorescence intensity was monitored during

continous TST at a single wavelength, with the integration time of 30 seconds and the gap of 30 seconds for adding the ligand, with slow but sufficient magnetic stirring to ensure mixing and keeping the temperature constant in the whole volume. During the gap the UV xenon flash lamp was switched off, to avoid photobleaching the sample. The cuvette has not been touched during the whole TST experiment to ensure constant geometry for the optical measurements. Titrations were performed at several eIF4E concentrations (0.05 μM–1 μM), in steady-state conditions provided by preincubation in the buffer of the appropriate pH and ionic strength. Aliquots (1 μl) of increasing concentrations (1 μM to 5 mM) of a ligand were added to 1400 μl of eIF4E solution. Suitable data correction was applied when the final dilution was ≥2% (but always ≤3.2%). Each titration consisted of 28–45 data points with a suitable number within the range, at which the total ligand concentration ([L]) was close to the concentration of eIF4E ([P_{act}]) (Figure 3). The curvature of the fitted function in this range mostly influences the accuracy of K_{as} to be determined.

Numerical data analysis

Theoretical curve for the fluorescence intensity (F) as a function of [L] was fitted to the experimental data points according to equation:

$$F = F(0) - [cx](\Delta\phi + \phi_{lig\text{-}free}) + [L]\phi_{lig\text{-}free}$$

where the equilibrium concentration of the cap–eIF4E complex [cx] is given by:

$$[cx] = \frac{[L] + [P_{act}]}{2} + \frac{1 - \sqrt{(K_{as}([L] - [P_{act}]) + 1)^2 + 4K_{as}[P_{act}]}}{2K_{as}}$$

The parameters to be extracted from the fit were as follows: K_{as}, the association constant; [P_{act}], the concentration of the active protein; $\Delta\phi = \phi_{P\text{-}act\text{-}free} - \phi_{cx}$, difference between the fluorescence efficiencies of the apo-protein and the complex; $\phi_{lig\text{-}free}$, the fluorescence efficiency of the free cap analogue in the solution; $F(0)$, the initial fluorescence intensity. The latter two parameters were independently verified experimentally. Total quenching was calculated as: $Q = F(0) - F(\infty) = [P_{act}]\Delta\phi$. For the peptides, $\phi_{lig\text{-}free}$ was fixed as zero, since the tyrosine fluorescence was eliminated. The fluorescence intensities (F) were corrected for the inner filter effect.[86] Its influence was negligible for the specific cap analogues but could change K_{as} values ~twofold for the weakly interacting and strongly absorbing cap analogues. The final K_{as} were calculated as a weighted average of 3–12 independent titration series, except for m^7GTP, for which more than 30 titration experiments were performed, in order to make statistical analysis of the method and as control for each protein batch. The control results were consistent within 10%. Eadie–Hofstee representation was not used, for its basic assumption of a great excess of the ligand in relation to the protein is not satisfied for molecular systems of a higher affinity (when $K_{as} \sim 10 \times 10^6\ M^{-1}$, saturation of ~40% occures already for $[L] \leq [P_{act}]$, at typical [P_{act}] ~ 0.1 μM). This makes the data nonlinear, even after corrections for dilution, inner filter effect, and free ligand emission.

Regressions were performed by means of non-linear, least-squares method, using ORIGIN 6.0 from Microcal Software Inc., USA. Statistical analysis were done on the basis of runs test and goodness of fit (R^2), not less than 0.999 for cap analogues and 0.99 for peptides. Discrimination between investigated models was based of the Snedecor's F-test, with the significance level assumed as $P < 0.05$.[87] All errors were calculated according to the propagation rules[88] on the basis of the numerical uncertainty resulting from the fitting.

The Gibbs free energy of binding ($\Delta G^\circ = -RT \ln K_{as}$) was calculated either from the binding constants K_{as}, or from $K_{as}^{(micro)}$ in case of the symmetrical cap analogues.

Interaction of eIF4E–cap in presence of electrolyte

Increase of the KCl concentration is accompanied by an increasing osmolality (2φ[KCl]) and decrease of the activity coefficient of water (a_w):

$$\log(a_w) = -\frac{2\varphi[KCl]}{\ln 10\Omega}$$

where $\varphi = 0.91 \pm 0.01$ is an approximately constant osmotic coefficient of KCl (0–0.5 M), and Ω is the number of moles of free solvent water in 1 kg of the solution. The latter is not assumed to be constant, but the presence of other buffer components of the molecular masses μ_i at the concentrations c_i, and the hydration number of KCl ($v \approx 5$),[89] are taken into account:

$$\Omega = \frac{1000 - \mu_{KCl}[KCl] - \sum \mu_i c_i}{\mu_{H_2O}} - v[KCl]$$

Keeping constant $\Omega = -55.5$ yields overestimation of the hydration effects (ΔN) by ~18%.

(1) Davies-Stockes-Robinson electrostatic screening approach.[59,60] Binding of two ions of opposite charges (protein z_1, and ligand z_2) is screened by the ionic atmosphere of the excess salt and other ionized components of the solution. The influence of ionic strength and osmotic stress on the activity coefficients of the interacting species leads to the expression:

$$\log(K_{as}) = \log(K_{as}(0)) + \frac{2Az_1z_2\sqrt{I}}{1 + a_jB\sqrt{I}} + \Delta N \log(a_w)$$

where ionic strength $I = [KCl] + \sum c_i z_i^2$, z_i is a charge of the ith species, a_j is a sum of radii of interacting species, and ΔN is a number of water molecules taken up to the macromolecular surfaces upon complex formation. The temperature-dependent coefficients at 20 °C are: $A = 0.50585$, $B = 0.32789$.[59]

(2) In terms of Wyman linkage analysis,[61] hydration effects and ionic interactions are considered stoichiometrically:

$$\log(K_{as}) = \log(K_{as}^0) - c \log(a_{KCl}) + \Delta N \log(a_w)$$

Thermodynamic activity of potassium cations (a_{KCl}) is used. Assuming $a_{KCl} = [KCl]$ leads to underestimation of the K_{as} value extrapolated to 1 M KCl by ~twofold. K_{as}^0 corresponds to the value of K_{as}, when the thermodynamic effects of cation release ($\log([KCl]) = 0$ at 1 M KCl) and of the hydration ($\log(a_w) = 0$ at 0 M KCl) cancel each other out. K_{as}^0 occurs at the KCl concentration of approximately 0.3 M. The contribution of the electrolyte effect (ΔG°_{el}) to the stability of the cap–eIF4E complex can be calculated as:

$$\Delta G^\circ_{el} = -SK_{as}RT \ln[KCl]$$

from the derivative:[55]

$$SK_{as} = \left(\frac{\partial \log K_{as}}{\partial \log[KCl]} \right)_{T,p} = -c - \Delta N \frac{2\phi[KCl]}{\Omega}$$

and the entropy of the electrolyte effect was calculated as:

$$\Delta S^{\circ}_{el} = -\frac{\Delta G^{\circ}_{el}}{T}$$

Ionic equilibria in eIF4E–cap complex

From Wyman analysis:

$$\log(K_{as}) = \log(K_{as}^{pH-ind}) - \log(1 + 10^{pH-pK_L}) - \log(1 + 10^{pK_P-pH})$$

the intrinsic, pH-independent association constant for the cationic ligand and the protein with anionic Glu103 (K_{as}^{pH-ind}), the effective acidic dissociation constant for the ligand in the presence of the protein (pK_L) and for Glu103 in the presence of the cap (pK_P), and pH optimal for binding ($pH_{opt} = (pK_L + pK_P)/2$) were obtained.

Thermodynamics of eIF4E binding to m^{7}GTP

The temperature dependence of K_{as} for m^{7}GTP was analysed according to the van't Hoff isobaric equation, assuming the entropy change ΔS° and the enthalpy change ΔH° as constants parameters over the whole range of temperatures:

$$\ln K_{as} = \frac{1}{R}\left(\Delta S^{\circ} - \frac{\Delta H^{\circ}}{T}\right)$$

Crystallography

Murine eIF4E (residues 28–217) was expressed in *E. coli*, purified from inclusion bodies by affinity chromatography using 7-methyl-GpppG during the elution, and crystallized as reported previously.[11] Diffraction data were collected from a single crystal at the Cornell High Energy Synchrotron Source using the A1 beamline and processed using DENZO and SCALEPACK,[90] yielding a 97.8% complete, sevenfold redundant data set from 20.0–1.8 Å resolution with an overall $R_{sym}(I) = 10.3\%$. The crystals were isomorphous with our 7-methyl-GDP–eIF4E cocrystals[11]. Difference electron density maps revealed unambiguous density for the 7-methyl-guanosine and three phosphate groups (Figure 5). The structure was refined using CNS yeilding a final crystallographic R factor of 22.4% and free R factor of 25.2%, with RMSDs on bond lengths and angles of 0.006 Å and 1.24°, respectively. The current refined model consists of eIF4E residues 36–206 and 212–217 plus 7-methyl-Gppp (complex 1), eIF4E residues 28–217 plus 7-methyl-Gppp (complex 2), and 186 water molecules. Atomic coordinates have been submitted to the PDB, accession no. 1L8B.

Acknowledgments

We are indebted to Lidia Chlebicka and Lilia Zhukova for the eIF4E expression and purification, and Wojciech Augustyniak, Mariusz Tasior and Monika Garas for helpful assistance in peptide synthesis. This work was supported partially by Human Frontier Science Program RG-0303/198-M, Polish Comittee for Scientific Research KBN 6 P04A 055 17, BST-718/BF, BW-1452, BW-1483/16, and US–Polish Maria Sklodowska-Curie Joint Fund II MEN/NSF-98-337. A.-C.G. was supported by Canadian Institutes for Health Research studentship. S.K.B. is an Investigator in the Howard Hughes Medical Institute.

References

1. Muthukrishnan, S., Both, G. W., Furuichi, Y. & Shatkin, A. J. (1975). 5′-Terminal 7-methylguanosine in eukaryotic mRNA is required for translation. *Nature*, **255**, 33–37.
2. Sonenberg, N. (1988). Cap-binding proteins of eukaryotic messenger RNA: functions in initiation and control of translation. *Prog. Nucl. Acid Res. Mol. Biol.* **35**, 173–207.
3. Konarska, M. M., Padgett, R. A. & Sharp, P. A. (1984). Recognition of cap structure in splicing *in vitro* of mRNA precursors. *Cell*, **38**, 731–736.
4. Izaurralde, E., Lewis, J., McGuigan, C., Jankowska, M., Darzynkiewicz, E. & Mattaj, I. W. (1994). A nuclear cap binding protein complex involved in pre-mRNA splicing. *Cell*, **78**, 657–668.
5. Izaurralde, E., Stepinski, J., Darzynkiewicz, E. & Mattaj, I. W. (1992). A cap binding protein that may mediate nuclear export of RNA polymerase II-transcribed RNAs. *J. Cell Biol.* **118**, 1287–1295.
6. Sonenberg, N. (1996). mRNA 5′ cap-binding protein eIF4E and control of cell growth. In *Translational Control* (Hershey, J. W. B., Mathews, M. B. & Sonenberg, N., eds), pp. 245–269, Cold Spring Harbor Laboratory Press, Cold Spring Harbor, NY.
7. Hentze, M. W. (1997). eIF4G: a multipurpose ribosome adapter? *Science*, **275**, 500–501.
8. Sachs, A. B., Sarnow, P. & Hentze, M. W. (1997). Starting at the beginning, middle, and end: translation initiation in eukaryotes. *Cell*, **89**, 831–838.
9. Imataka, H., Gradi, A. & Sonenberg, N. (1998). A newly identified N-terminal amino acid sequence of human eIF4G binds poly(A)-binding protein and functions in poly(A)-dependent translation. *Eur. Mol. Biol. Org. J.* **17**, 7480–7489.
10. Gradi, A., Imataka, H., Svitkin, Y. V., Rom, E., Raught, B., Morino, S. & Sonenberg, N. (1998). A novel functional human eukaryotic translation initiation factor 4G. *Mol. Cell. Biol.* **18**, 334–342.
11. Marcotrigiano, J., Gingras, A. C., Sonenberg, N. & Burley, S. K. (1997). Cocrystal structure of the messenger RNA 5′ cap-binding protein (eIF4E) bound to 7-methyl-GDP. *Cell*, **89**, 951–961.
12. Matsuo, H., Li, H., McGuire, A. M., Fletcher, C. M., Gingras, A. C., Sonenberg, N. & Wagner, G. (1997). Structure of translation factor eIF4E bound to m7GDP and interaction with 4E-binding protein. *Nature Struct. Biol.* **4**, 717–724.
13. McCubbin, W. D., Edery, I., Altmann, M., Sonenberg, N. & Kay, C. M. (1988). Circular dichroism and fluorescence studies on protein synthesis initiation factor eIF-4E and two mutant forms from the yeast *Saccharomyces cerevisiae*. *J. Biol. Chem.* **263**, 17663–17671.
14. Carberry, S. E., Rhoads, R. E. & Goss, D. J. (1989). A spectroscopic study of the binding of m7GTP and m7GpppG to human protein synthesis initiation factor 4E. *Biochemistry*, **28**, 8078–8083.

15. Ueda, H., Maruyama, H., Doi, M., Inoue, M., Ishida, T., Morioka, H. *et al.* (1991). Expression of a synthetic gene for human cap binding protein (human IF-4E) in *Escherichia coli* and fluorescence studies on interaction with mRNA cap structure analogues. *J. Biochem. (Tokyo)*, **109**, 882–889.
16. Morino, S., Yasui, M., Doi, M., Inoue, M., Ishida, T., Ueda, H. & Uesugi, S. (1994). Direct expression of a synthetic gene in *Escherichia coli*: purification and physicochemical properties of human initiation factor 4E. *J. Biochem. (Tokyo)*, **116**, 687–693.
17. Hagedorn, C. H., Spivak-Kroizman, T., Friedland, D. E., Goss, D. J. & Xie, Y. (1997). Expression of functional eIF-4E human: purification, detailed characterization, and its use in isolating eIF-4E binding proteins. *Protein Expt. Purif.* **9**, 53–60.
18. Wieczorek, Z., Niedzwiecka-Kornas, A., Chlebicka, L., Jankowska, M., Kiraga, K., Stepinski, J. *et al.* (1999). Fluorescence studies on association of human translation initiation factor eIF4E with mRNA cap-analogues. *Z. Naturforsch. [C.]*, **54**, 278–284.
19. Niedzwiecka-Kornas, A., Chlebicka, L., Stepinski, J., Jankowska-Anyszka, M., Wieczorek, Z., Darzynkiewicz, E. *et al.* (1999). Spectroscopic studies on association of mRNA cap-analogues with human translation factor eIF4E. From modelling of interactions to inhibitory properties. *Collect. Symp. Ser.* **2**, 214–218.
20. Hsu, P. C., Hodel, M. R., Thomas, J. W., Taylor, L. J., Hagedorn, C. H. & Hodel, A. E. (2000). Structural requirements for the specific recognition of an m7G mRNA cap. *Biochemistry*, **39**, 13730–13736.
21. Cai, A., Jankowska-Anyszka, M., Centers, A., Chlebicka, L., Stepinski, J., Stolarski, R. *et al.* (1999). Quantitative assessment of mRNA cap analogues as inhibitors of *in vitro* translation. *Biochemistry*, **38**, 8538–8547.
22. Gingras, A. C., Raught, B. & Sonenberg, N. (1999). eIF4 initiation factors: effectors of mRNA recruitment to ribosomes and regulators of translation. *Annu. Rev. Biochem.* **68**, 913–963.
23. Raught, B. & Gingras, A. C. (1999). eIF4E activity is regulated at multiple levels. *Int. J. Biochem. Cell Biol.* **31**, 43–57.
24. Haghighat, A., Mader, S., Pause, A. & Sonenberg, N. (1995). Repression of cap-dependent translation by 4E-binding protein 1: competition with p220 for binding to eukaryotic initiation factor-4E. *Eur. Mol. Biol. Org. J.* **14**, 5701–5709.
25. Mader, S., Lee, H., Pause, A. & Sonenberg, N. (1995). The translation initiation factor eIF-4E binds to a common motif shared by the translation factor eIF-4 gamma and the translational repressors 4E-binding proteins. *Mol. Cell. Biol.* **15**, 4990–4997.
26. Altmann, M., Schmitz, N., Berset, C. & Trachsel, H. (1997). A novel inhibitor of cap-dependent translation initiation in yeast: p20 competes with eIF4G for binding to eIF4E. *Eur. Mol. Biol. Org. J.* **16**, 1114–1121.
27. Pause, A., Belsham, G. J., Gingras, A. C., Donze, O., Lin, T. A., Lawrence, J. C., Jr & Sonenberg, N. (1994). Insulin-dependent stimulation of protein synthesis by phosphorylation of a regulator of 5′-cap function. *Nature*, **371**, 762–767.
28. Poulin, F., Gingras, A. C., Olsen, H., Chevalier, S. & Sonenberg, N. (1998). 4E-BP3, a new member of the eukaryotic initiation factor 4E-binding protein family. *J. Biol. Chem.* **273**, 14002–14007.
29. Marcotrigiano, J., Gingras, A. C., Sonenberg, N. & Burley, S. K. (1999). Cap-dependent translation initiation in eukaryotes is regulated by a molecular mimic of eIF4G. *Mol. Cell*, **3**, 707–716.
30. Gingras, A. C., Gygi, S. P., Raught, B., Polakiewicz, R. D., Abraham, R. T., Hoekstra, M. F. *et al.* (1999). Regulation of 4E-BP1 phosphorylation: a novel two-step mechanism. *Genes Dev.* **13**, 1422–1437.
31. Gingras, A. C., Raught, B., Gygi, S. P., Niedzwiecka, A., Miron, M., Burley, S. K. *et al.* (2001). Hierarchical phosphorylation of the translation inhibitor 4E-BP1. *Genes Dev.* **15**, 2852–2864.
32. Mothe-Satney, I., Brunn, G. J., McMahon, L. P., Capaldo, C. T., Abraham, R. T. & Lawrence, J. C., Jr (2000). Mammalian target of rapamycin-dependent phosphorylation of PHAS-I in four (S/T)P sites detected by phospho-specific antibodies. *J. Biol. Chem.* **275**, 33836–33843.
33. Karim, M. M., Hughes, J. M., Warwicker, J., Scheper, G. C., Proud, C. G. & McCarthy, J. E. (2001). A quantitative molecular model for modulation of mammalian translation by the eIF4E-binding protein 1. *J. Biol. Chem.* **276**, 20750–20757.
34. Mothe-Satney, I., Yang, D., Fadden, P., Haystead, T. A. & Lawrence, J. C., Jr (2000). Multiple mechanisms control phosphorylation of PHAS-I in five (S/T)P sites that govern translational repression. *Mol. Cell. Biol.* **20**, 3558–3567.
35. Gingras, A. C., Raught, B. & Sonenberg, N. (2001). Regulation of translation initiation by FRAP/mTOR. *Genes Dev.* **15**, 807–826.
36. Ptushkina, M., von der Haar, T., Karim, M. M., Hughes, J. M. & McCarthy, J. E. (1999). Repressor binding to a dorsal regulatory site traps human eIF4E in a high cap-affinity state. *Eur. Mol. Biol. Org. J.* **18**, 4068–4075.
37. Ptushkina, M., von der Haar, T., Vasilescu, S., Frank, R., Birkenhager, R. & McCarthy, J. E. (1998). Cooperative modulation by eIF4G of eIF4E-binding to the mRNA 5′ cap in yeast involves a site partially shared by p20. *Eur. Mol. Biol. Org. J.* **17**, 4798–4808.
38. von der Haar, T., Ball, P. D. & McCarthy, J. E. (2000). Stabilization of eukaryotic initiation factor 4E binding to the mRNA 5′-cap by domains of eIF4G. *J. Biol. Chem.* **275**, 30551–30555.
39. Guruprasad, K., Reddy, B. V. & Pandit, M. W. (1990). Correlation between stability of a protein and its dipeptide composition: a novel approach for predicting *in vivo* stability of a protein from its primary sequence. *Protein Eng.* **4**, 155–161.
40. Shibata, S., Morino, S., Tomoo, K., In, Y. & Ishida, T. (1998). Effect of mRNA cap structure on eIF-4E phosphorylation and cap binding analyses using Ser209-mutated eIF-4Es. *Biochem. Biophys. Res. Commun.* **247**, 213–216.
41. Kentsis, A., Dwyer, E. C., Perez, J. M., Sharma, M., Chen, A., Pan, Z. Q. & Borden, K. L. (2001). The ring domains of the promyelocytic leukemia protein PML and the arenaviral protein Z repress translation by directly inhibiting translation initiation factor eIF4E. *J. Mol. Biol.* **312**, 609–623.
42. Lodish, H. F. (1974). Model for the regulation of mRNA translation applied to haemoglobin synthesis. *Nature*, **251**, 385–388.
43. Chu, L. Y. & Rhoads, R. E. (1980). Inhibition of cell-free messenger ribonucleic acid translation by 7-methylguanosine 5′-triphosphate: effect of messenger ribonucleic acid concentration. *Biochemistry*, **19**, 184–191.

44. Duncan, R., Milburn, S. C. & Hershey, J. W. (1987). Regulated phosphorylation and low abundance of HeLa cell initiation factor eIF-4F suggest a role in translational control. Heat shock effects on eIF-4F. *J. Biol. Chem.* **262**, 380–388.
45. Rau, M., Ohlmann, T., Morley, S. J. & Pain, V. M. (1996). A reevaluation of the cap-binding protein, eIF4E, as a rate-limiting factor for initiation of translation in reticulocyte lysate. *J. Biol. Chem.* **271**, 8983–8990.
46. Hiremath, L. S., Webb, N. R. & Rhoads, R. E. (1985). Immunological detection of the messenger RNA cap-binding protein. *J. Biol. Chem.* **260**, 7843–7849.
47. Haghighat, A. & Sonenberg, N. (1997). eIF4G dramatically enhances the binding of eIF4E to the mRNA 5′-cap structure. *J. Biol. Chem.* **272**, 21677–21680.
48. Wieczorek, Z., Stepinski, J., Jankowska, M. & Lonnberg, H. (1995). Fluorescence and absorption spectroscopic properties of RNA 5′-cap analogues derived from 7-methyl-N2,7-dimethyl- and N2,N2,7-trimethyl-guanosines. *J. Photochem. Photobiol. B*, **28**, 57–63.
49. Hu, G., Gershon, P. D., Hodel, A. E. & Quiocho, F. A. (1999). mRNA cap recognition: dominant role of enhanced stacking interactions between methylated bases and protein aromatic side chains. *Proc. Natl Acad. Sci. USA*, **96**, 7149–7154.
50. Hodel, A. E., Gershon, P. D., Shi, X. & Quiocho, F. A. (1996). The 1.85 Å structure of vaccinia protein VP39: a bifunctional enzyme that participates in the modification of both mRNA ends. *Cell*, **85**, 247–256.
51. Quiocho, F. A., Hu, G. & Gershon, P. D. (2000). Structural basis of mRNA cap recognition by proteins. *Curr. Opin. Struct. Biol.* **10**, 78–86.
52. Raught, B., Gingras, A. C. & Sonenberg, N. (2000). Regulation of ribosomal recruitment in eukaryotes. In *Translational Control of Gene Expression* (Sonenberg, N., Hershey, J. W. B. & Mathews, M. B., eds), pp. 245–293, Cold Spring Harbor Laboratory Press, Cold Spring Harbor, NY.
53. Hu, C. Q., Sturtevant, J. M., Thomson, J. A., Erickson, R. E. & Pace, C. N. (1992). Thermodynamics of ribonuclease T1 denaturation. *Biochemistry*, **31**, 4876–4882.
54. Pace, C. N., Shirley, B. A., McNutt, M. & Gajiwala, K. (1996). Forces contributing to the conformational stability of proteins. *FASEB J.* **10**, 75–83.
55. Record, M. T., Jr, Ha, J. H. & Fisher, M. A. (1991). Analysis of equilibrium and kinetic measurements to determine thermodynamic origins of stability and specificity and mechanism of formation of site-specific complexes between proteins and helical DNA. *Methods Enzymol.* **208**, 291–343.
56. Parsegian, V. A., Rand, R. P. & Rau, D. C. (2000). Osmotic stress, crowding, preferential hydration, and binding: a comparison of perspectives. *Proc. Natl Acad. Sci. USA*, **97**, 3987–3992.
57. Parsegian, V. A., Rand, R. P. & Rau, D. C. (1995). Macromolecules and water: probing with osmotic stress. *Methods Enzymol.* **259**, 43–94.
58. Chaires, J. B., Satyanarayana, S., Suh, D., Fokt, I., Przewloka, T. & Priebe, W. (1996). Parsing the free energy of anthracycline antibiotic binding to DNA. *Biochemistry*, **35**, 2047–2053.
59. Davies, C. W. (1962). *Ion Association*, Butterworths, London.
60. Robinson, R. A. & Stokes, R. H. (1970). *Electrolyte Solutions*, Butterworths, London.
61. Wyman, J., Jr (1964). Linked functions and reciprocal effects in hemoglobin: a second look. *Advan. Protein Chem.*, 223–286.
62. Dawson, R. M., Elliott, D. C., Elliott, W. H. & Jones, K. M. (1969). Data for Biochemical Research, vol. 2, Clarendon Press, Oxford pp. 174–175.
63. Hempel, R., Schmidt-Brauns, J., Gebinoga, M., Wirsching, F. & Schwienhorst, A. (2001). Cation radius effects on cell-free translation in rabbit reticulocyte lysate. *Biochem. Biophys. Res. Commun.* **283**, 267–272.
64. Blachut-Okrasinska, E., Bojarska, E., Niedzwiecka, A., Chlebicka, L., Darzynkiewicz, E., Stolarski, R. *et al.* (2000). Stopped-flow and Brownian dynamics studies of electrostatic effects in the kinetics of binding of 7-methyl-GpppG to the protein eIF4E. *Eur. Biophys. J.* **29**, 487–498.
65. Pyronnet, S., Imataka, H., Gingras, A. C., Fukunaga, R., Hunter, T. & Sonenberg, N. (1999). Human eukaryotic translation initiation factor 4G (eIF4G) recruits mnk1 to phosphorylate eIF4E. *Eur. Mol. Biol. Org. J.* **18**, 270–279.
66. Waskiewicz, A. J., Johnson, J. C., Penn, B., Mahalingam, M., Kimball, S. R. & Cooper, J. A. (1999). Phosphorylation of the cap-binding protein eukaryotic translation initiation factor 4E by protein kinase Mnkl *in vivo*. *Mol. Cell Biol.* **19**, 1871–1880.
67. Scheper, G. C., van Kollenburg, B., Hu, J., Luo, Y., Goss, D. J. & Proud, C. G. (2002). Phosphorylation of eukaryotic initiation factor 4E markedly reduces its affinity for capped mRNA. *J. Biol. Chem.* **277**, 3303–3309.
68. Ha, J. H., Capp, M. W., Hohenwalter, M. D., Baskerville, M. & Record, M. T., Jr (1992). Thermodynamic stoichiometries of participation of water, cations and anions in specific and non-specific binding of lac repressor to DNA. Possible thermodynamic origins of the glutamate effect on protein–DNA interactions. *J. Mol. Biol.* **228**, 252–264.
69. Colombo, M. F., Rau, D. C. & Parsegian, V. A. (1992). Protein solvation in allosteric regulation: a water effect on hemoglobin. *Science*, **256**, 655–659.
70. Colombo, M. F., Rau, D. C. & Parsegian, V. A. (1994). Reevaluation of chloride's regulation of hemoglobin oxygen uptake: the neglected contribution of protein hydration in allosterism. *Proc. Natl Acad. Sci. USA*, **91**, 10517–10520.
71. Qu, X. & Chaires, J. B. (2001). Hydration changes for DNA intercalation reactions. *J. Am. Chem. Soc.* **123**, 1–7.
72. Record, M. T., Jr, Anderson, C. F. & Lohman, T. M. (1978). Thermodynamic analysis of ion effects on the binding and conformational equilibria of proteins and nucleic acids: the roles of ion association or release, screening, and ion effects on water activity. *Q. Rev. Biophys.* **11**, 103–178.
73. Saenger, W. (1987). Structure and dynamics of water surrounding biomolecules. *Annu. Rev. Biophys. Biophys. Chem.* **16**, 93–114.
74. Rhoads, R. E., Hellmann, G. M., Remy, P. & Ebel, J. P. (1983). Translational recognition of messenger ribonucleic acid caps as a function of pH. *Biochemistry*, **22**, 6084–6088.
75. Niedzwiecka-Kornas, A., Chlebicka, L., Jankowska-Anyszka, M., Stepinski, J., Dadlez, M., Gingras, A.C. *et al.* (1999). RNA Meeting Abstract'99.
76. Miyoshi, H., Youtani, T., Ide, H., Hori, H., Okamoto, K., Ishikawa, M. *et al.* (1999). Binding analysis of *Xenopus laevis* translation initiation factor 4E (eIF4E)

in initiation complex formation. *J. Biochem. (Tokyo)*, **126**, 897–904.
77. Darzynkiewicz, E., Ekiel, I., Tahara, S. M., Seliger, L. S. & Shatkin, A. J. (1985). Chemical synthesis and characterization of 7-methylguanosine cap analogues. *Biochemistry*, **24**, 1701–1707.
78. Jankowska, M., Stepinski, J., Stolarski, R., Temeriusz, A. & Darzynkiewicz, E. (1993). Synthesis and properties of new NH_2 and N7 substituted GMP and GTP 5′-mRNA cap analogues. *Collect. Czech. Chem. Commun.* **58**, 138–141.
79. Darzynkiewicz, E., Stepinski, J., Ekiel, I., Jin, Y., Haber, D., Sijuwade, T. & Tahara, S. M. (1988). Beta-globin mRNAs capped with m7G, m2.7(2)G or m2.2.7(3)G differ in intrinsic translation efficiency. *Nucl. Acids Res.* **16**, 8953–8962.
80. Stepinski, J., Bretner, M., Jankowska, M., Felczak, K., Stolarski, R., Wieczorek, Z. *et al.* (1995). Synthesis and properties of P^1,P^2-, P^1,P^3- and P^1,P^4-dinucleotide di-, tri- and tetraphosphate mRNA 5′-cap analogues. *Nucleosides Nucleotides*, **14**, 717–721.
81. Jankowska, M., Stepinski, J., Stolarski, R., Wieczorek, Z., Temeriusz, A., Haber, D. & Darzynkiewicz, E. (1996). H-1 NMR and fluorescence studies of new mRNA 5′-cap analogues. *Collect. Czech. Chem. Commun.* **61**, 197–202.
82. Darzynkiewicz, E., Stepinski, J., Tahara, S. M., Stolarski, R., Ekiel, I., Haber, D. *et al.* (1990). Synthesis, conformation and hydrolytic stability of P^1,P^3-dinucleoside triphosphate groups related to mRNA 5′-cap, and comparative kinetic studies on their nucleoside and nucleoside monophosphate analogues. *Nucleosides Nucleotides*, **9**, 599–618.
83. Edery, I., Altmann, M. & Sonenberg, N. (1988). High-level synthesis in *Escherichia coli* of functional cap-binding eukaryotic initiation factor eIF-4E and affinity purification using a simplified cap-analogue resin. *Gene*, **74**, 517–525.
84. Schnolzer, M., Alewood, P., Jones, A., Alewood, D. & Kent, S. B. (1992). *In situ* neutralization in Boc-chemistry solid phase peptide synthesis. Rapid, high yield assembly of difficult sequences. *Int. J. Pept. Protein Res.* **40**, 180–193.
85. Wakamiya, T., Saruto, K., Yasuoka, J. & Kusumoto, S. (1994). An efficient procedure for solid-phase synthesis of phosphopeptides by Fmoc strategy. *Chem. Letters*, 1099–1102.
86. Parker, C. A. (1968). *Photoluminescence of Solutions*, Elsevier, Amsterdam.
87. Beyer, W. H. (1987). *CRC Standard Mathematical Tables*, vol. 28, p. 536, CRC Press, Boca Raton, FL.
88. Taylor, J. R. (1982). *An Introduction to Error Analysis*, University Science Books, Mill Valley, CA.
89. Marcus, Y. (1997). *Ion Properties*, Marcel Dekker, New York.
90. Otwinowski, Z. & Minor, W. (1997). Processing of X-ray diffraction data collected in oscillation mode. *Methods Enzymol.* **276**, 307–326.

Edited by J. Doudna

(Received 21 November 2001; received in revised form 25 March 2002; accepted 5 April 2002)